ACS ES&T Air

Open Access

pubs.acs.org/estair

Article

Increasing Contributions of Temperature-Dependent Oxygenated Organic Aerosol to Summertime Particulate Matter in New York City

Tori Hass-Mitchell, Taekyu Joo, Mitchell Rogers, Benjamin A. Nault, Catelynn Soong, Mia Tran, Minguk Seo, Jo Ellen Machesky, Manjula Canagaratna, Joseph Roscioli, Megan S. Claflin, Brian M. Lerner, Daniel C. Blomdahl, Pawel K. Misztal, Nga L. Ng, Ann M. Dillner, Roya Bahreini, Armistead Russell, Jordan E. Krechmer, Andrew Lambe, and Drew R. Gentner*

Cite This: *ACS EST Air* 2024, 1, 113−128

Read Online

ACCESS | Metrics & More | Article Recommendations | Supporting Information

ABSTRACT: As part of the summer 2022 NYC-METS (New York City metropolitan Measurements of Emissions and TransformationS) campaign and the ASCENT (Atmospheric Science and Chemistry mEasurement NeTwork) observational network, speciated particulate matter was measured in real time in Manhattan and Queens, NY, with additional gas-phase measurements. Largely due to observed reductions in inorganic sulfate aerosol components over the 21st century, summertime aerosol composition in NYC has become predominantly organic (80−83%). Organic aerosol source apportionment via positive matrix factorization showed that this is dominated by secondary production as oxygenated organic aerosol (OOA) source factors comprised 73−76% of OA. Primary factors, including cooking-related organic aerosol (COA) and hydrocarbon-like organic aerosol (HOA) comprised minor fractions of OA, only 13−15% and 10−11%, respectively. The two sites presented considerable spatiotemporal variations in OA source factor concentrations despite similar average $PM_{2.5}$ concentrations. The less- and more-oxidized OOA factors exhibited clear temperature dependences at both sites with increased concentrations and greater degrees of oxidation at higher temperatures, including during a heatwave. With strong temperature sensitivity and minimal changes in summertime concentrations since 2001, secondary OA poses a particular challenge for air quality policy in NYC that will very likely be exacerbated by continued climate change and extreme heat events.

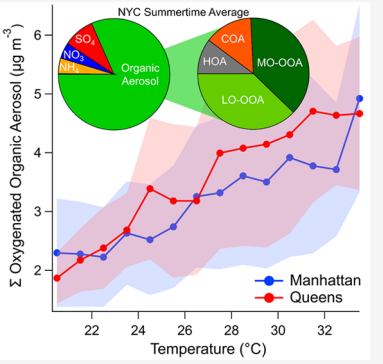

KEYWORDS: *urban air quality, atmospheric chemistry, organic aerosol, aerosol mass spectrometry, particulate matter, climate change, heatwave events*

1. INTRODUCTION

Atmospheric aerosols, including $PM_{2.5}$ (particulate matter with diameter ≤ 2.5 μm), are major air pollutants of concern given their human health effects and influence on climate.[1,2] Prominent inorganic aerosol components include sulfate (SO_4^{2-}), nitrate (NO_3^-), and ammonium (NH_4^+). Organic aerosols generally comprise a large but variable fraction of total $PM_{2.5}$, with contributions from primary (i.e., directly emitted) and secondary organic aerosol (POA, SOA).[3] The current $PM_{2.5}$ air quality standard in the US is 12 μg m^{-3} (3-year annual average) with 5 μg m^{-3} recommended by the WHO.[4] Yet, there is evidence for health effects below 5 μg m^{-3} and for SOA having the strongest influence on cardiorespiratory disease mortality.[2,5] SOA is formed across both local and regional scales from the oxidation of volatile organic compounds (VOCs) as well as intermediate volatility and semivolatile organic compounds (IVOCs, SVOCs) in either the gas or suspended aqueous phase.[6−8] These VOCs-SVOCs are emitted locally and regionally from a diverse mix of biogenic and anthropogenic sources, even in urban areas where successful reductions in motor vehicle-related emissions have resulted in a larger role for non-traditional sources (e.g., volatile chemical products; VCPs).[9−12]

New York City is a densely populated megacity that has historically struggled with air pollution, including PM; NYC is currently in attainment for $PM_{2.5}$, but remains in nonattainment for ozone (8-hour standard: 70 ppb; Figure 1b).[13] Although $PM_{2.5}$ concentrations in NYC have decreased over the 21st century, there has been minimal decline in the last decade (Figure 1a), with some variability across major sites (Figure S2). Yet, the most recent intensive summertime aerosol-focused campaigns in NYC were last conducted in 2001 and 2009 (at the Queens College ground site, shown in

Received: September 8, 2023
Revised: December 18, 2023
Accepted: December 19, 2023
Published: January 22, 2024

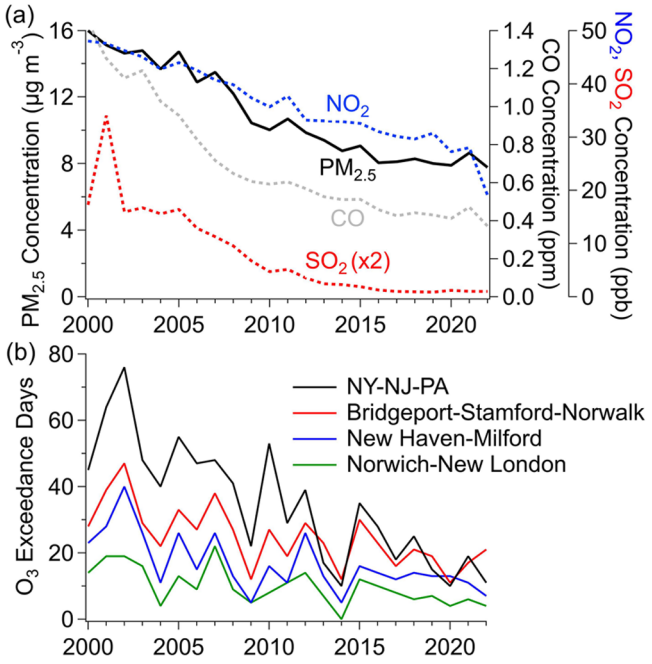

Figure 1. (a) Average annual $PM_{2.5}$ concentrations in NYC across 2000−2022, shown with CO, SO_2, and NO_2 for comparison (see Figure S1 for a map of regulatory monitoring sites used and Table S1 for a list). (b) Number of ozone exceedance days per year in the NYC metropolitan ("NY-NJ-PA") region and in progressively downwind coastal Connecticut areas.

Figure 2). These campaigns utilized Aerodyne Aerosol Mass Spectrometers (AMS)[14] for in situ aerosol speciation and subsequent positive matrix factorization (PMF)[15] to examine aerosol source factors and their contributions in NYC for the first time, reporting a distributed mix of organic and inorganic aerosol components and source factors (discussed further below).[16−19] In comparison, wintertime measurements were made relatively more recently in 2015 via aircraft during the Wintertime INvestigation of Transport, Emissions, and Reactivity (WINTER) campaign and reported that the majority (58%) of wintertime organic aerosol is secondary in nature and originated from anthropogenic pollution sources.[20,21] In 2018, the Long Island Sound Tropospheric Ozone Study (LISTOS) further examined anthropogenic VOC concentrations and ozone production, including from VCP-related sources.[11,12,22,23] In addition to these intensive measurement campaigns, monitoring networks with sites in NYC (e.g., National Core (NCore), Chemical Speciation Network (CSN)) and other targeted measurement sites across multiple NYC boroughs have monitored concentrations of $PM_{2.5}$, SO_4^{2-}, NO_3^-, NH_4^+, organic carbon (OC), elemental carbon (EC), and other gas-phase species of interest. These networks have produced long-term data sets with intermittent sampling, and associated studies have examined trends and contributing factors from 2000 to 2018, reporting contributions from a mix of local and regional sources influencing air quality in NYC.[24−27]

Despite NYC being the largest U.S. city and one of the largest metropolitan areas in the world, summertime intensive air quality campaigns focused on aerosols with chemically-detailed research instrumentation have been less frequent than other U.S. cities (e.g., Los Angeles, Houston).[20,28] Thus, the overall objective of this study was to examine the present-day aerosol composition, contributing sources, factors, and environmental conditions during summer 2022 as part of NYC-METS (New York City metropolitan Measurements of Emissions and TransformationS) and ASCENT (Atmospheric Science and Chemistry mEasurement NeTwork) efforts. The specific goals were to (1) measure speciated aerosol concentrations at two sites in Manhattan and Queens, along

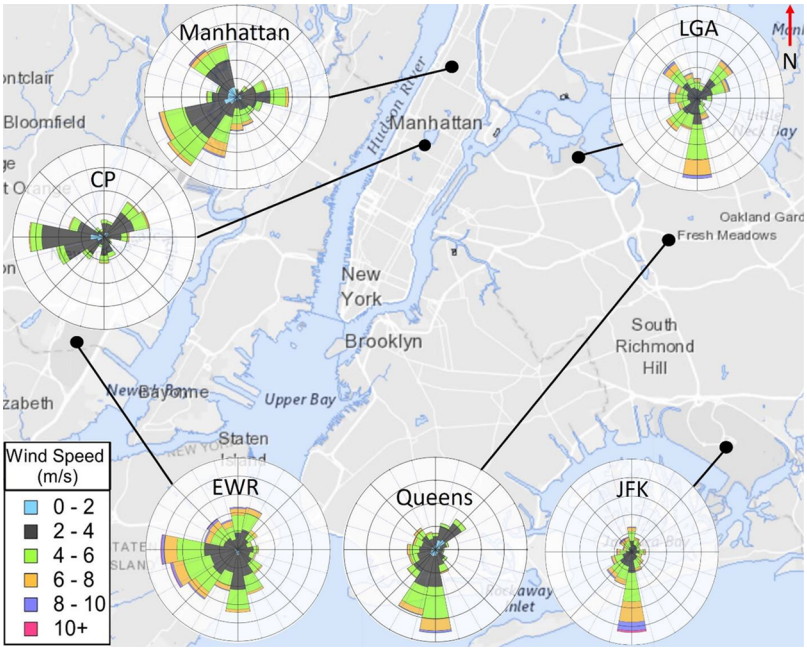

Figure 2. Summertime (June−August) wind rose plots at long-term monitoring sites measured from 2000−2022 (JFK, LGA, and EWR airports, and Central Park (CP)), shown with 2020−2022 data from Manhattan and Queens. Calm wind speeds (i.e., <1 m/s) were excluded for all sites. Summertime 2020−2022 wind data from the Bronx NYSDEC site can be found in Figure S3; data from this site were used for comparison to measurements made in Manhattan during the measurement intensive. Map data reprinted with permission from USGS 2022.

https://doi.org/10.1021/acsestair.3c00037
ACS EST Air 2024, 1, 113−128

with associated measurements of gases and meteorology, to characterize the chemical and environmental conditions influencing aerosols at both sites; (2) conduct OA source apportionment using PMF to investigate contributing source factors at each site; (3) examine temporal (e.g., diurnal) patterns and site-to-site variability in aerosol species, OA source factors, and gas-phase species associated with aerosol emissions or chemical processes; (4) evaluate the influence of meteorology and environmental conditions on OA concentrations and source factors at both sites; and (5) compare summer 2022 observations to prior studies (e.g., 2001, 2009) to examine the evolution of aerosol composition in NYC and inform potential air quality mitigation efforts under evolving policies and climate.

2. METHODS

2.1. Sampling Sites and Instrumentation. This study utilizes measurements from two sites that are a part of the ASCENT observational network (ascent.research.gatech.edu) and NYC-METS 2022 ground site intensive, which was part of the broader AGES+/AEROMMA (Atmospheric Emissions and Reactions Observed from Megacities to Marine Areas) campaigns.[29] The summer measurement intensive examined here took place from July 8th to August 7th, 2022. The NYC-METS site is located at the Advanced Science Research Center (ASRC) at the City University of New York (CUNY) in upper Manhattan (85 St. Nicholas Terrace, 40.82°N, 73.95°W, 89 m above sea level), which is the same location as prior measurements conducted in 2020−21.[12,23] Aerosol instruments shared the same 1/4 in. copper inlet and a $PM_{2.5}$ cyclone followed by a Nafion dryer. The ASCENT site is located at the New York State Department of Environmental Conservation (NYSDEC) in Queens College (40.74°N, 73.82°W, 16.2−16.6 m above sea level), the same location as prior measurements in 2001 and 2009,[16−19] including the first ACSM test deployment.[30] The aerosol instruments at Queens had independent inlets that were coupled with respective $PM_{2.5}$ cyclones and 1/2 in. stainless steel inlets with Nafion dryers (5.2−5.6 m above ground). The Manhattan and Queens sites are located 14 km apart. The Manhattan site is located 1.1 km due east of the Hudson River and 27 km north of the Atlantic Ocean, and the Queens site is located 18 km north of the ocean. The Manhattan site is in a very densely populated area and thus in close proximity to a diverse array of urban sources, while the Queens site is a long-established urban background site (following typical siting rules) relatively proximal to nearby highways. Select measurements unavailable at the Manhattan site (e.g., filter measurements, formaldehyde, NO_y) were used from a Bronx NYSDEC site located 8 km NE of the Manhattan site, making it often directly downwind.

Aerosol Chemical Speciation Monitor (ACSM). The Aerodyne Time-of-Flight (TOF) ACSMs, present at both the Manhattan and Queens sites, were used to measure mass concentration and chemical composition of nonrefractory aerosols (i.e., organic, nitrate, ammonium, sulfate, and chloride), with a mass resolution of 168 in Manhattan and 244 in Queens.[31−33] Both instruments utilized standard vaporizer configurations with the NYC-METS ACSM using a PM_1 lens in Manhattan and the ASCENT ACSM using a $PM_{2.5}$ lens in Queens (following ASCENT protocol; SOPs available online at https://ascent.research.gatech.edu/instrumentation). Although the deployment of a standard vaporizer with a $PM_{2.5}$ inlet caused lower collection efficiency at size range between 1 and 2.5 μm,[34] alternatively deploying a capture vaporizer, which was developed to achieve unit collection efficiency by minimizing particle bounce, would cause higher rates of aerosol fragmentation due to increased thermal decomposition,[35−37] so this study compares instruments both with standard vaporizers. Each ACSM was connected to a $PM_{2.5}$ cyclone (3 lpm), and a Nafion dryer was placed upstream to dry the particles (RH < 35%). The preliminary real-time data was collected and displayed with Acquility (v2.3.18). The data, saved as Tofwerk-formatted HDF files, was processed and analyzed with the Tofware v3.2.4, operated in IgorPro (Wavemetrics). The analysis was based on the work from Fröhlich et al.[31] with one key difference. While the instrument was operated in "fast-mode" (1 s data collected),[38] the data was collected in 40 s packets (20 s ambient, 20 s particle filter) and either saved at 80 s for Manhattan or at 10 min for Queens ACSM data, with additional averaging in data processing. The ionization efficiency (IE) for nitrate and relative ionization efficiency (RIE) for ammonium and sulfate for ACSMs were calibrated at the beginning and end of the experiment with 300 nm ammonium nitrate and ammonium sulfate (Table S2). Further discussion of hardware, calibration parameters, data processing, data validation, and instrument uptimes is detailed in Section S1.

Aethalometer. The AE33 aethalometer from Magee Scientific, present at both sites, was used to measure black carbon (BC) concentrations at 1 min resolution, following ASCENT protocol. The instrument measured optical absorption at wavelengths of 370, 470, 520, 590, 660, 880, and 950 nm. The BC concentrations used in this study were determined using absorption measured at 880 nm, assuming a mass absorption cross-section coefficient of 7.77 $m^2\ g^{-1}$.

In Situ Gas-Phase Measurements of Organic Compounds at NYC-METS Manhattan Site. In situ gas-phase measurements were also deployed to the NYC-METS Manhattan site and included in this analysis to support aerosol measurements by investigating VOC sources that impact gas-phase chemistry, ozone production, and aerosol production. A TOFWERK/Aerodyne Vocus proton transfer reaction (PTR) TOF-MS measured gas-phase compounds in the VOC-SVOC range at high time resolution (e.g., 1 Hz) using hydronium (H_3O^+) reagent ions with a high resolution (HR) TOF mass analyzer with a resolution of 10 Hz.[39] VOCs were sampled from a 1/2 in. PFA inlet at 90 m ASL with a subsecond residence time. Detected compounds were quantified using a calibration gas mixture containing 14 common VOCs, and additional compounds were quantified with known H_3O^+ reaction rates.[40] An in situ Aerodyne GC-TOF also measured select VOCs (i.e., benzene and toluene) using a dedicated inlet at 88 m ASL at 30 min resolution following the methods in Claflin et al.[41] An iodide adduct high-resolution time-of-flight chemical ionization mass spectrometer (HR-TOF-CIMS) measured multifunctional organic and inorganic gaseous compounds[42,43] via a dedicated PFA inlet at 87 m ASL. For this analysis, ion counts s^{-1} were used in place of calibrated mixing ratios.

Other Supporting Measurements. A range of criteria pollutant or other gas-phase measurements were used in this analysis as tracers of combustion sources, chemical processes, and/or atmospheric dilution. Ozone was measured via 2B-Tech 202 and Teledyne API T400 ozone analyzers in Manhattan and Queens, respectively. Nitrogen oxides were measured as NO + NO_2 via a 2B-Tech 405 monitor at the Manhattan site. Supporting gas-phase measurements at the

https://doi.org/10.1021/acsestair.3c00037
ACS EST Air 2024, 1, 113−128

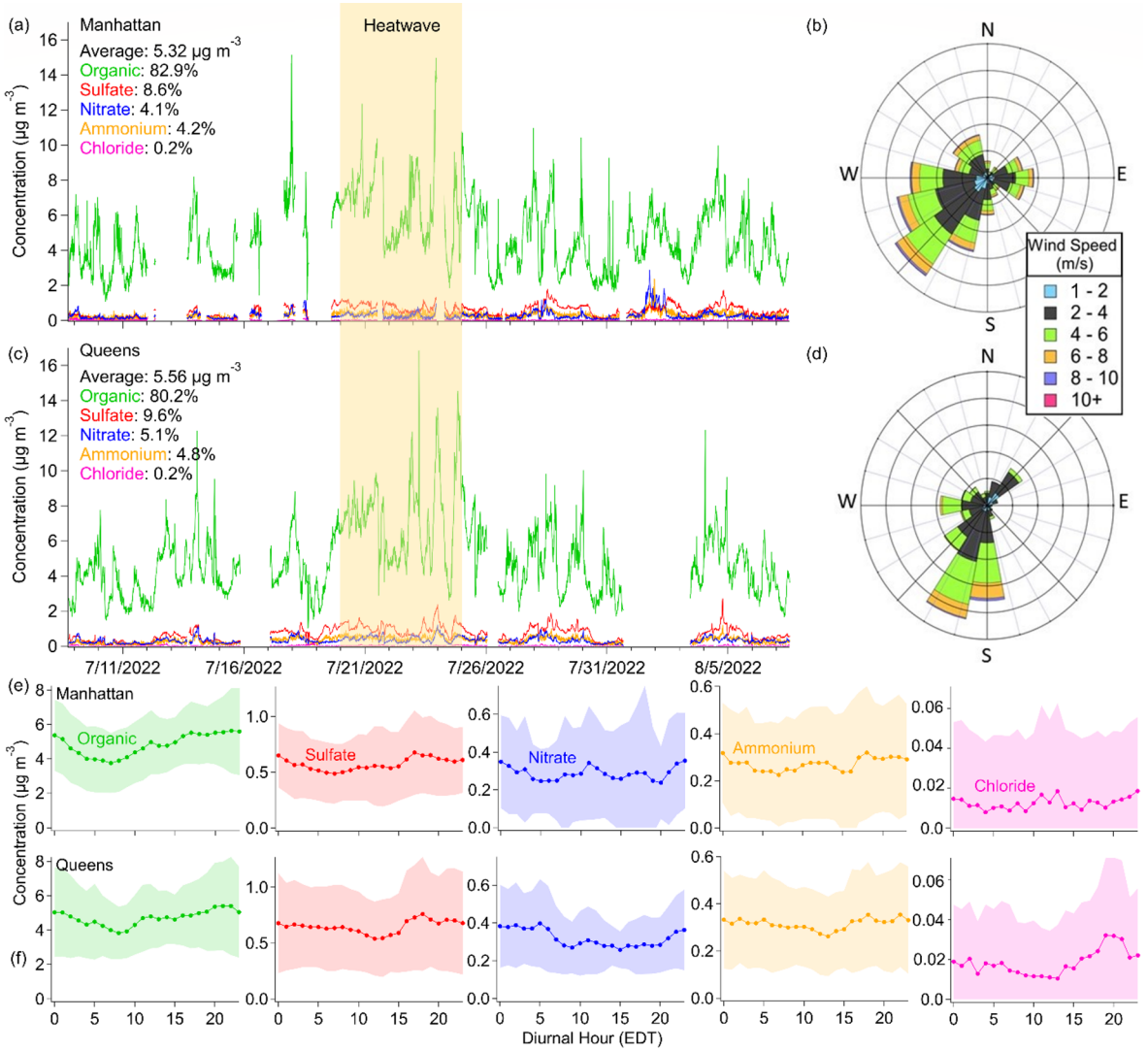

Figure 3. Non-refractory aerosol mass concentrations measured by TOF-ACSM in (a) Manhattan and (c) Queens during the summer intensive campaign period. Legends in (a) and (c) show average PM mass loadings and relative percentage of each nonrefractory aerosol component; associated masses are shown in Table 1. Inorganic concentrations are shown in greater detail in Figure S5. Accompanying diurnal profiles are shown in (e) and (f), with shading representing one sigma standard deviation. Respective wind roses are shown for Manhattan (b) and Queens (d) during the campaign period.

Manhattan site had a 1/4 in. PFA inlet colocated with the ACSM inlet. Nitrogen oxides were also measured at the Queens site and in the Bronx, with each site having two different instruments, one measuring total nitrogen oxides (i.e., NO_y) with an inlet mounted catalyst (Thermo Scientific Model 42*i*-Y NO_y Analyzer), and the second measuring NO_x (i.e., NO + NO_2; Thermo Scientific Model 42*i*-TL TRACE Level NO_x Analyzer). The ratio of NO_x/NO_y was used as a photochemical clock for atmospheric aging. A 5% offset was observed between NO concentrations on the NO_x and NO_y instruments in Queens and attributed to calibration factor differences; this offset was adjusted for in the NO_x/NO_y ratio. SO_2 was measured via a Thermo Fisher analyzer (TEI 43i - TLE). Carbon monoxide (CO) was measured via an Aerodyne tunable infrared laser direct absorption spectroscopy (TILDAS)[44] in Manhattan and a Thermo Fisher analyzer (TEI 48i - TLE) in Queens. Formaldehyde was measured at the NYSDEC Bronx site via a Picarro G2307 Gas Concentration Analyzer. Meteorological data, including wind direction and speed, were collected in Manhattan via a RM Young model 81000 ultrasonic anemometer. Meteorological data for the Queens site were provided by NYS Mesonet and collected via Lufft V200A sonic anemometer.[45] A Vaisala HMP155 relative humidity and temperature sensor was also employed at both sites.

2.2. Source Apportionment via Positive Matrix Factorization (PMF) Analysis. PMF is a source apportionment tool that is widely applied to OA spectral matrices obtained via ACSM or AMS.[15,30,37,46,47] It is a receptor-only multivariate factor analytical model that solves bilinear unmixing problems. The observed data matrix is deconvolved as a linear combination of various factors with constant mass spectra but varying concentrations across the dataset. PMF was performed on unit mass resolution (UMR) OA mass spectra (m/z 12−100) obtained via ACSM at both sites. OA data matrices were generated using Tofware v3.2.4 and pretreated using the PMF Evaluation Toolkit (PET v.3.08). Variables with a signal-to-noise ratio lower than 2.5 were removed, while variables with a signal-to-noise ratio between 2.5 and 5 were downweighted by a factor of 2. The errors related to CO_2^+ ($m/$

https://doi.org/10.1021/acsestair.3c00037
ACS EST Air 2024, 1, 113−128

z 44; i.e., O^+ (m/z 16), HO^+ (m/z 17), H_2O^+ (m/z 18), and CO^+ (m/z 28)) signals were downweighted to avoid excessive CO_2^+ weighting. Diagnostic plots are shown in Figure S4.

3. RESULTS AND DISCUSSION

3.1. Overview of Meteorology, Diurnal Patterns, and Variations between Sites. Summertime meteorological conditions in NYC were influenced by a frequent sea breeze effect with southerly onshore flows often approaching from the Atlantic Ocean and Atlantic coast with westerly winds intermittently bringing inflow from upwind states (e.g., Pennsylvania, New Jersey, upstate New York).[48,49] However, local wind directions varied considerably throughout NYC with major differences between sites on Long Island compared to Manhattan and nearby New Jersey over multidecadal summertime (June−August) observations (Figure 2). These long-term records at major airports on Long Island (JFK, LGA) showed prevailing S−SSW flows similar to the Queens measurement site (2020−2022), while Newark's EWR airport and the Manhattan site showed more frequent SW−W influence (Figure 2). Summer 2022 exhibited similar wind conditions as prior years at both sites with afternoon wind speed maxima that were relatively faster in Queens (Figures 3 and S6). Yet, prevailing wind patterns varied expectedly at other times of year (i.e., wintertime).[12,23] Average temperatures and RH were 26.9 ± 3.14°C and 61.9 ± 15.0% in Manhattan and 26.8 ± 3.15°C and 64.4 ± 15.1% in Queens, where the standard deviations included here and hereafter represent the 1σ spread of the observations. During July 20−24, the greater NYC area experienced a heatwave where daily maxima reached 33−35°C. In general, higher temperatures were not associated with slower wind speeds, including during the heatwave period (i.e., <0.1% decrease in wind speeds on average during the heatwave; Figure S7), and there were only minor differences in incoming wind directions at the Queens site compared to the rest of the campaign period with no major difference observed in the distributions of backward trajectories (Figures S7 and S8).

Average concentrations of aerosol components and associated gas-phase measurements are summarized for both sites in Table 1. Despite evident spatiotemporal heterogeneity in PM concentrations between sites (Figures S2 and S10), average total loadings observed by the ACSMs were similar, with 5.90 ± 1.93 $\mu g\ m^{-3}$ in Manhattan and 6.09 ± 1.99 $\mu g\ m^{-3}$ in Queens (Table 1). Although the sites trended together (Figure 3), aerosol concentrations and relative composition varied dynamically between sites due to differences in meteorological conditions, topography, local sources, and chemical transformations (Figures 3 and S8). Wind direction-dependent variations were observed for some particle- and gas-phase species, based on concentration wind roses and directional percentiles (Figures S11 and S12).

The diurnal cycles of aerosol components were relatively consistent between Manhattan and Queens (Figure 3e,f). Both sites showed morning OA minima with increasing concentrations starting 8:00−9:00 EDT (LT) that steadily increased through the evening as the result of multiple OA source factors (discussed below). Sulfate showed a distinctly different diurnal cycle than prior observations.[17,19] For both Manhattan and Queens, sulfate concentrations were relatively stable on average during the morning and early afternoon, with evening maxima (16:00−20:00) and minor overnight enhancements. Prior observations showed a more pronounced early afternoon peak (~13:00−14:00) when sulfate comprised a larger fraction of PM.[17,19] This difference in diurnal patterns might have been associated with a transition from predominantly local to regional sulfate sources (Section 3.2). Nitrate exhibited a generally flat diurnal profile despite some variations between sites (Figure 3), potentially caused by differences in upwind NO_x emissions and/or chemistry (e.g., nitric acid production and ammonium nitrate formation equilibrium). The Queens diurnal profile showed elevated nighttime concentrations (22:00−5:00), followed by a distinct maximum (10:00−12:00), which was overall in agreement with prior observations from 2001 and 2009.[17,19] Ammonium's diurnal profile corresponded to the summed nitrate and sulfate diurnal profiles in both Manhattan and Queens (Figure 3), as ammonium is one of the most abundant cations in the atmosphere, and nitrate and sulfate are among the most prevalent atmospheric anions. Chloride diurnal profiles varied between sites and showed patterns distinct from prior observations.[19] Chloride in Manhattan showed relatively stable diurnal average concentrations, whereas chloride in Queens peaked in the evening (19:00−21:00).

Table 1. Average Overall Concentrations (Average ± One Standard Deviation) of Aerosol Components, Select Gas-Phase Compounds of Interest, and Near-Source Photochemical Clock Ratios within the City during the Intensive Observational Period (July 8 to August 7, 2022)[a]

	Manhattan	Queens
Aerosol Components ($\mu g\ m^{-3}$)		
Organics	4.41 ± 1.86	4.45 ± 1.91
MO-OOA	1.63 ± 1.03	1.24 ± 0.84
LO-OOA	1.16 ± 0.57	1.73 ± 0.93
COA	0.58 ± 0.43	0.49 ± 0.32
HOA	0.40 ± 0.27	0.38 ± 0.28
Sulfate	0.46 ± 0.35	0.54 ± 0.42
Nitrate	0.22 ± 0.16	0.29 ± 0.15
Ammonium	0.22 ± 0.17	0.27 ± 0.21
Chloride	0.011 ± 0.013	0.013 ± 0.019
Black Carbon	0.58 ± 0.33	0.53 ± 0.28
Total[b]	5.90 ± 1.93	6.09 ± 1.99
Select Gas-Phase Compounds (ppb)		
O_3 8 h Max	55 ± 10	53 ± 12
O_3 1 h Max	64 ± 16	60 ± 14
NO	1.56 ± 1.26	0.70 ± 0.92
NO_2	9.54 ± 6.93	8.78 ± 4.69
SO_2	0.23 ± 0.19	0.16 ± 0.16
CO	240 ± 72	208 ± 57
HCHO	1.67 ± 1.34[c]	
Photochemical Clocks (Compound Ratios)		
NO_x/NO_y	0.96 ± 0.10[c]	0.98 ± 0.068
Toluene/Benzene	1.54 ± 0.81	
C8 Aromatics/Benzene	1.25 ± 0.54	
C9 Aromatics/Benzene	0.91 ± 0.34	

[a]Notes: All concentrations are reported as geometric means with one sigma standard deviation, while photochemical clock ratios are reported as arithmetic means with one sigma standard deviation. Corresponding arithmetic means of aerosol component concentrations are included in Table S3. Distributions of aromatic/benzene ratios can be found in Figure S9. Instrument configurations and PM size ranges for aerosol components are detailed in Sections 2.1 and S1. [b]Total = Organics + Sulfate + Nitrate + Ammonium + Chloride + Black Carbon. [c]denotes measurements made at a monitoring station in the Bronx (NYSDEC site, 40.87°N, 73.88°W).

https://doi.org/10.1021/acsestair.3c00037
ACS EST Air 2024, 1, 113−128

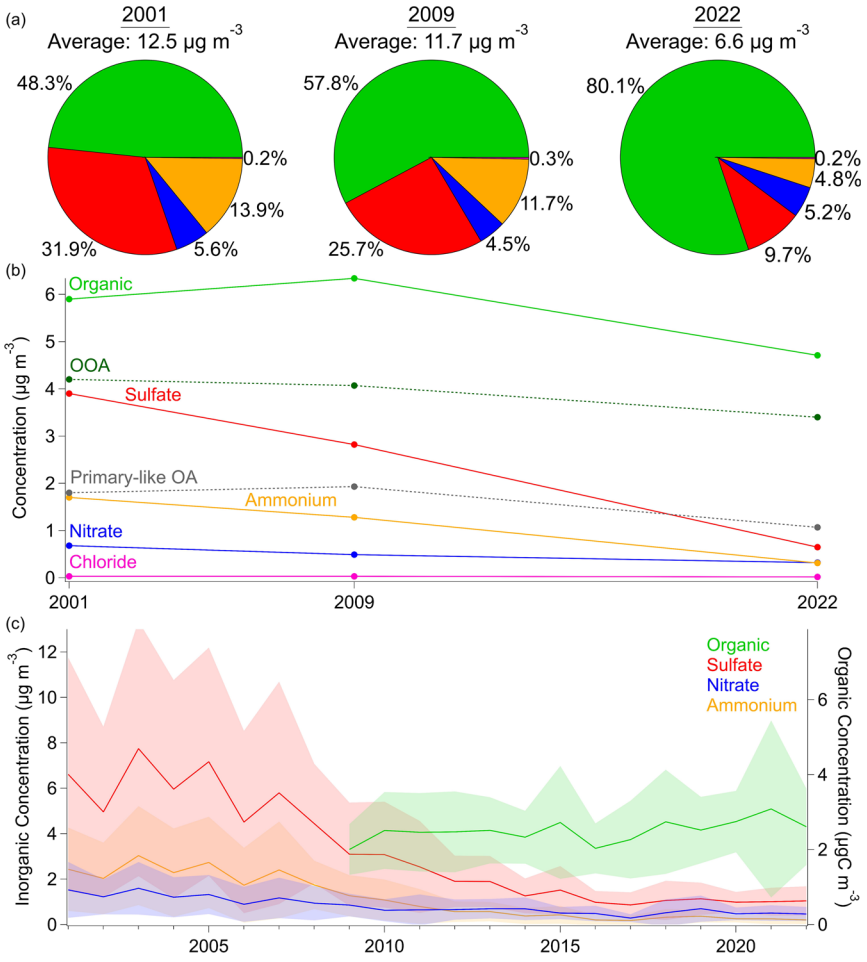

Figure 4. Historical evolution of PM composition in NYC. (a) Summertime nonrefractory aerosol composition measured via aerosol mass spectrometry at the Queens site in 2001, 2009, and 2022 (this study). Average PM loading was measured by AMS in 2001 and 2009,[17,19] while in 2022 it includes average ACSM and black carbon aethalometer measurements. (b) Trends in average aerosol component concentrations and summed OA source factor contributions measured in Queens from studies in panel (a). Based on differentiated factors in the prior studies, the "primary-like OA" trace includes only HOA in 2001, while in 2009 and 2022, it includes both HOA and COA. Means and compositional percentages for 2022 data presented in panels (a) and (b) are based on arithmetic means (Table S3) calculated for comparison to prior measurements. (c) Summertime average (± one standard deviation) aerosol mass concentrations measured by the CSN (2001−2022) at the same Queens site. Organic data is shown from 2009 to 2022 only due to a change in protocol in measuring OC by the CSN in 2008.[74] Organic aerosol concentration (right) is shown in ugC m^{-3}; the right axis is scaled to provide an approximate visual comparison to the left (ug m^{-3}) based on OA compositional ratios (O/C, H/C) measured via AMS in 2009.[19] Additional comparisons to CSN data are included in Figures S13 and S14.

3.2. Increasing Relative Contributions of Organic Aerosol. Average aerosol loadings observed via ACSM were substantially lower than prior studies at the Queens site (12.5 $\mu g\ m^{-3}$ in 2001, 11.7 $\mu g\ m^{-3}$ in 2009, 6.6 $\mu g\ m^{-3}$ in 2022),[17,19] consistent with declining total $PM_{2.5}$ concentrations in the NYC metropolitan region since 2000 (Figure 1a). Organics constituted the largest fraction of summertime PM in both Manhattan and Queens, representing 80−83% of observed non-refractory aerosol mass on average, followed by sulfate (9−10%), nitrate (4−5%), ammonium (4−5%), and chloride (0.2%) (Figures 3 and 4; Table 1). The overwhelming dominance of organics at present day stands in contrast to previous studies (48% in 2001, 58% in 2009). With only minor reductions in POA since 2001 (Figure 4b), this shift can be attributed to decreasing contributions of sulfate (9−10% of aerosol in 2022) compared to prior studies (26% in 2009, 32% in 2001). The successful decline in $PM_{2.5}$ via sulfate is a result of regional and national SO_2 emissions reductions, as shown by declining SO_2 concentrations in the region since 2000 (Figure 1a) as well as an 83% decrease in nonrefractory sulfate aerosol concentrations (Figure 4, measured via AMS in 2001 and ACSM in 2022) with 2022 summertime average concentrations of 160−230 ppt on average at the two sites (Table 1). This trend of relatively stagnant organics with comparatively greater gains in inorganic aerosol reductions in online high-resolution data (Figure 4a,b) was similarly observed in summertime $PM_{2.5}$ data from the Chemical Speciation Network (CSN) using periodic filters (Figure 4c) at Queens College and other NYC sites.

3.3. Organic Aerosol Source Apportionment at Manhattan and Queens Sites. Source apportionment of OA via PMF analysis yielded four unique source factors at each site (Figure 5), with each source factor exhibiting characteristic mass spectra and distinct diurnal patterns (see Table S4 for correlation analysis, and Section S2 for further discussion of PMF solutions). The OA source factors included more oxidized OOA (MO-OOA), less oxidized OOA (LO-OOA), cooking-related OA (COA), and hydrocarbon-like OA (HOA). Further discussion of each factor, including mass spectra, diurnal patterns, correlations with precursors or

https://doi.org/10.1021/acsestair.3c00037
ACS EST Air 2024, 1, 113−128

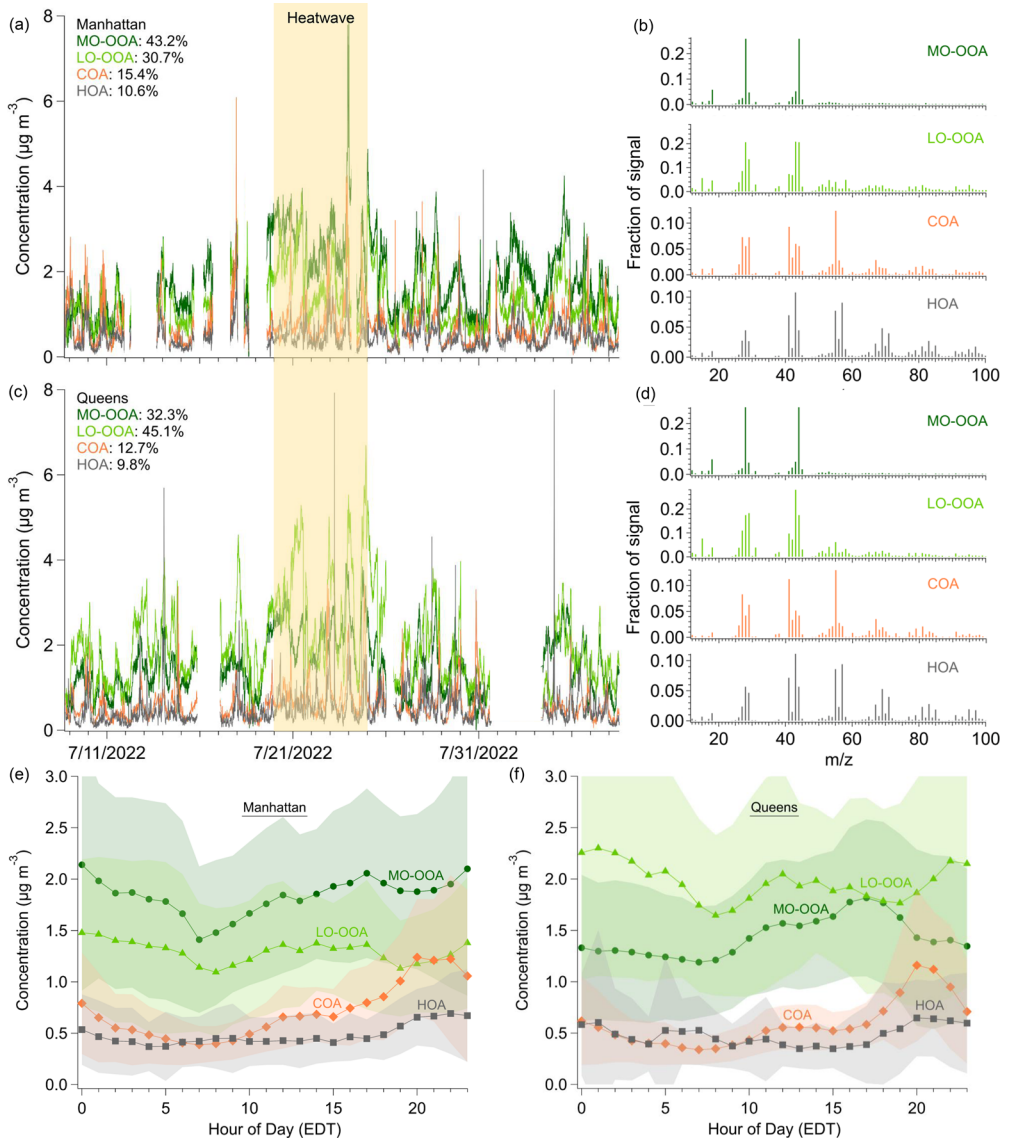

Figure 5. Summertime organic aerosol source apportionment results from Manhattan and Queens sites. Time series of OA factors during the summer intensive (a, c) along with their respective UMR mass spectral profiles (b, d) and diurnal profiles (e, f) for OA source factors in Manhattan and Queens. Additional relevant PMF diagnostic plots can be found in Figure S4, and individual source factor diurnals can be found in Figure S15.

otherwise related species, as well as potential influences from various sources, chemical processes, and meteorology, is provided in the following subsections as well as in Section S2, with comparison of variations in source factor contributions observed between the sites shown in Figure 6.

More- and Less-Oxidized Oxygenated Organic Aerosols (MO-OOA, LO-OOA). MO-OOA and LO-OOA emerged as major factors in the PMF solutions at both the Manhattan and Queens sites (Figure 5). Overall, MO-OOA comprised 43% of the OA in Manhattan (1.63 ± 1.03 $\mu g\ m^{-3}$) and 32% in Queens (1.24 ± 0.84 $\mu g\ m^{-3}$), while LO-OOA represented 31% of the OA in Manhattan (1.16 ± 0.57 $\mu g\ m^{-3}$) and 45% in Queens (1.73 ± 0.93 $\mu g\ m^{-3}$; Table 1). We note that the separation between MO-OOA and LO-OOA can be uncertain as the factors are distinguished by gradients in oxidation state rather than distinctive sources of emitted aerosol.[47,50−52] The sum of the OOA (i.e., MO-OOA + LO-OOA) comprised 77% of the total OA on average in Queens (74% in Manhattan). This greater OOA fraction represents an increase compared to 2009 measurements (64%),[19] which was likely influenced by reductions in primary-like OA emissions (Figure 4). This shift in composition was more marked considering that the ratio of total OOA to sulfate (Manhattan: 5.7, Queens: 5.3; Table 1) was over 4 times higher than previous observations in 2009 (Queens: 1.29),[19] highlighting the increasing role of OOA in summertime PM composition due to the greater reductions in sulfate precursors compared to OOA precursors.

The average diurnal patterns of total OOA were consistent between Manhattan and Queens with clear evidence of daytime production as well as nighttime enhancements (Figure 7a), though there was day-to-day variability (Figure 5a,c). The diurnal behavior of LO-OOA was similar between the two sites with slightly higher overall concentrations at the Queens site (Figure 5e,f and Table 1). Daytime enhancements in LO-OOA began at ∼9:00 on average and continued into the late afternoon (i.e., 17:00−18:00; Figure 5e,f). These daytime LO-OOA enhancements coincided with ozone and formaldehyde production beginning around 9:00 and broad average maxima

https://doi.org/10.1021/acsestair.3c00037
ACS EST Air 2024, 1, 113−128

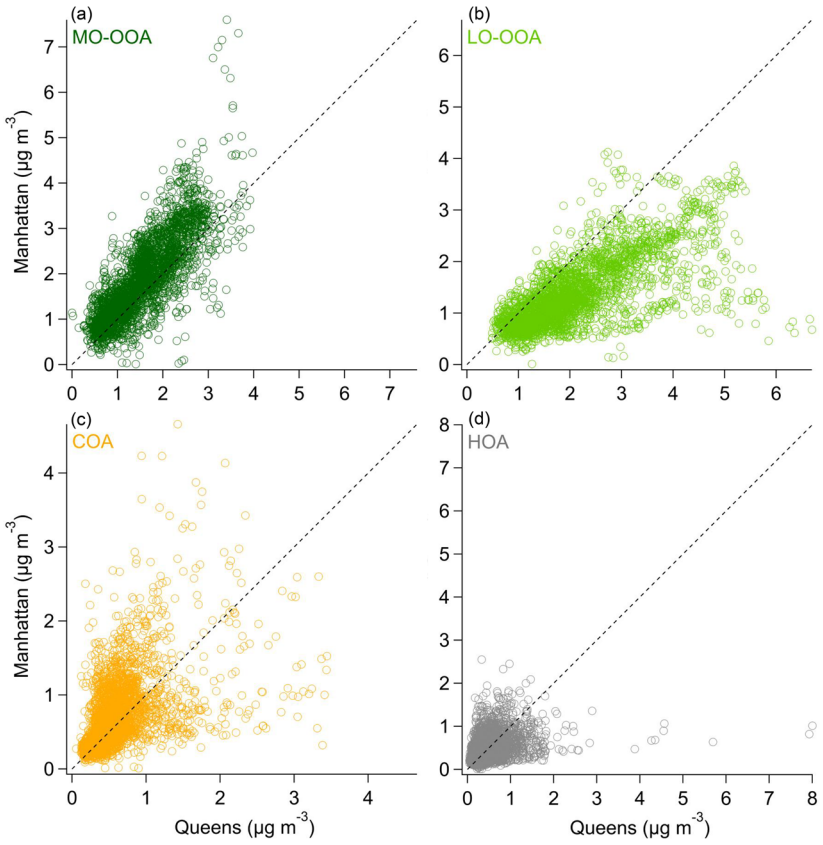

Figure 6. Comparison of OA source factor concentrations at Manhattan vs Queens at 10 min resolution for (a) MO-OOA, (b) LO-OOA, (c) COA, and (d) HOA, shown with 1:1 lines. Primary emissions (HOA, COA) in (c) and (d) exhibited the most variability between sites, yet spatiotemporal variability was also observed in LO-OOA and in Manhattan's larger MO-OOA enhancements.

in ozone (i.e., 12:00−19:00), formaldehyde (9:00−18:00), and photochemical clocks (e.g., NO_x/NO_y ratios), indicating aging of local emissions starting around 9:00−10:00 (Figure 7). MO-OOA concentrations began increasing at both sites in the morning (~7:00−9:00) with daytime average maxima around 17:00 (Figure 5e,f), similar to prior observations of a MO-OOA-like factor.[19] Nighttime MO-OOA varied between sites with more elevated average concentrations at night in Manhattan. There were also average daytime enhancements in Queens that could be associated with upwind MO-OOA production and/or transport occurring with elevated afternoon southerly wind speeds that coincided with Queens MO-OOA enhancements (Figures 5e,f and S6), similar to the S−SW back-trajectory clusters of a MO-OOA-like factor measured in 2009,[19] with more-aged OOA during this onshore flow. At both sites, the relative ratios of MO-OOA to LO-OOA increased across the daytime (e.g., 8:00 to 18:00), with some likely contributions from the continued oxidation of less-oxidized towards more-oxidized organic compounds in the aerosol phase, as seen in prior work with similar factors.[19]

Despite the close similarities between total OOA abundance and patterns at the two sites (Figure 7a), this intersite comparison revealed a few key differences (Figure 6). MO-OOA played a larger role at the Manhattan site with not only greater average abundances of MO-OOA and higher nighttime MO-OOA enhancements (Figure 5e), but also overall more aged OA and a slightly more oxidized LO-OOA factor, both evidenced by f_{44}/f_{43} ratios (Figures 5b,d and S19). This enhanced photochemistry was also shown in the greater afternoon ozone maxima that persisted longer into the afternoon in Manhattan compared to Queens (Figure 7b), as well as lower minima in the NO_x/NO_y ratios observed near the Manhattan site compared to Queens (Figure 7c). These variations in ozone/SOA production and OOA aging are partly influenced by differences in upwind emissions and chemical conditions in air parcels being transported across local and regional scales, as shown by the prevailing winds at each site (Figures 2 and 3b,d). While both sites were influenced by inflow from the south to southwest during the summer, the Queens site often experienced a sea breeze coming across Brooklyn and part of Queens to the site (with these air parcels seeing prior influence from the mid-Atlantic seaboard; Figure S20).[48] The areas upwind of the Manhattan site include more-densely populated parts of Manhattan and urban New Jersey, with an additional influence from terrestrial biogenic emissions upwind of the city. These variations highlight the spatiotemporal variability of OOA abundances across NYC and the role of wind direction (and speed) in background contributions, SOA and ozone precursor emissions, and oxidation conditions.

Cooking-Related and Hydrocarbon-Like Organic Aerosol (COA, HOA). Primary-like contributions from HOA (10−11%) and COA (13−15%) were responsible for smaller fractions of OA in NYC compared to secondary OOA factors (Figure 5). The average concentration of HOA was 0.40 ± 0.27 $\mu g\ m^{-3}$ in Manhattan and 0.38 ± 0.28 $\mu g\ m^{-3}$ in Queens, while the average concentration of COA was 0.58 ± 0.43 $\mu g\ m^{-3}$ in Manhattan and 0.49 ± 0.32 $\mu g\ m^{-3}$ in Queens.

HOA exhibited diurnal patterns that were relatively muted in Manhattan, with small nighttime enhancements (~0.1 $\mu g\ m^{-3}$; Figure 5e). At Queens, there was also a minor morning

https://doi.org/10.1021/acsestair.3c00037
ACS EST Air 2024, 1, 113−128

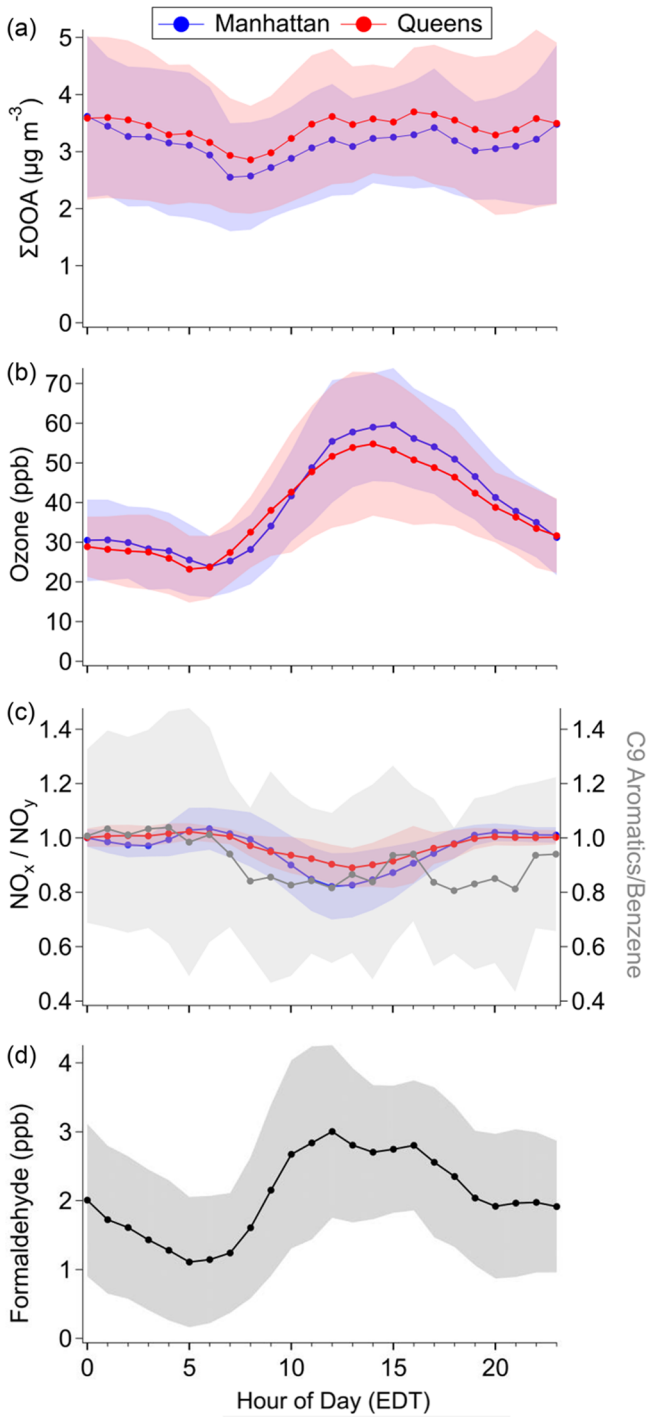

Figure 7. Products and indicators of oxidation chemistry. Diurnal profiles of (a) ΣOOA concentrations at Manhattan and Queens sites, (b) ozone at Manhattan and Queens sites, (c) photochemical clock ratios, including NO_x vs. NO_y measured in the Bronx (blue; NYSDEC site, 40.87°N, 73.88°W) and Queens (red), along with C_9 aromatics vs benzene for comparison measured at the Manhattan site, and (d) formaldehyde measured at the NYSDEC Bronx site. The CO-normalized ΣOOA diurnal can be found in Figure S16. The diurnal profile of nitric acid abundance (via I-CIMS) can be found in Figure S18 for comparison to NO_x/NO_y, highlighting 3× daytime enhancements following similar temporal trends.

peak from 5:00−8:00 that was similarly observed in the diurnal cycles of CO, NO_x, and BC, indicating the influence of local traffic-related emissions (Figure S20). This morning enhancement was more pronounced in Queens, potentially because the Queens site is located near multiple major highways.

COA exhibited clear diurnal patterns with a major peak in the evening (i.e., dinner times) and smaller yet evident enhancements starting midday with lunchtime cooking activities (Figure 5e,f). These diurnal patterns were largely consistent with prior observations in Queens, but at 42% lower concentrations,[19] suggesting potential localized reductions in COA-related emissions influencing the Queens site.

Compared to all other aerosol species and component source factors, COA was the only component that showed increased concentrations during weekends compared to weekdays, including when normalizing by CO to account for dilution (Tables S5 and S6). This suggests greater outdoor cooking activities over the weekend, similar to prior observations at other locations (e.g., greater Los Angeles[53]). For comparison, all other nonrefractory aerosol species showed decreased concentrations during weekends compared to weekdays, including when normalized by CO (Tables S5 and S6). All CO dilution-normalization calculations were made by normalizing each time-averaged concentration of the species of interest ($\mu g\ m^{-3}$) by the corresponding concentration of CO (ppb), as CO is commonly used to account for atmospheric dilution in and downwind of urban environments, acknowledging that CO is not co-emitted by all SOA precursor sources.[46] Both MO-OOA and LO-OOA showed decreased concentrations during weekends compared to weekdays (Tables S5 and S6); however, these reductions were not attributed to differences in historically studied weekend shifts (i.e., traffic changes) in VOC-SVOC precursor emissions since weekdays were significantly warmer by 0.3−0.4 °C on average. HOA in Manhattan showed no significant weekday vs weekend differences, while HOA in Queens exhibited a weekday enhancement of ∼10% (Tables S5 and S6), possibly suggesting increased weekday contributions from HOA-emitting vehicles at the Queens site. Additionally, there were only five weekends within the measurement intensive, and the changes were not consistently observed across all weekends (Figure 5).

Overall, the contribution of these primary-like OA factors has decreased compared to prior measurements in Queens, with HOA and COA decreasing by 47% and 42% since 2009, respectively.[19] While cooking-related emissions remain important for urban (and indoor) air quality given their mitigation challenges,[54] the reduction in COA concentrations suggests some reductions in COA source contributions at the Queens site since 2009,[19] though further studies are necessary to confirm this trend across larger spatial scales.

3.4. Organic Aerosol Temperature-Dependence. OA had a positive correlation with ambient temperature at both sites (Figure 8a). Despite differences in local emissions, OA chemical composition (Figures 5 and 6), meteorology, and transport (e.g., Figure 2), linear regressions demonstrated similar OA vs temperature profiles between Manhattan and Queens with slopes of 0.30 ± 0.02 and 0.28 ± 0.02 $\mu g\ m^{-3}\ °C^{-1}$, respectively (Figure 8a). For OA sampled during the summer intensive, this positive correlation with temperature was observed across a range of temporal resolutions, from 5−10 min (Figure 8a) to daily mean OA (Figure S21), eliminating the potential bias from diurnal temperature patterns. Sulfate and ammonium also had positive correlations with ambient temperature, while BC showed a weak trend with temperature (Figure S22). The correlation between OA and temperature was also observed in multi-year measurements

https://doi.org/10.1021/acsestair.3c00037
ACS EST Air 2024, 1, 113−128

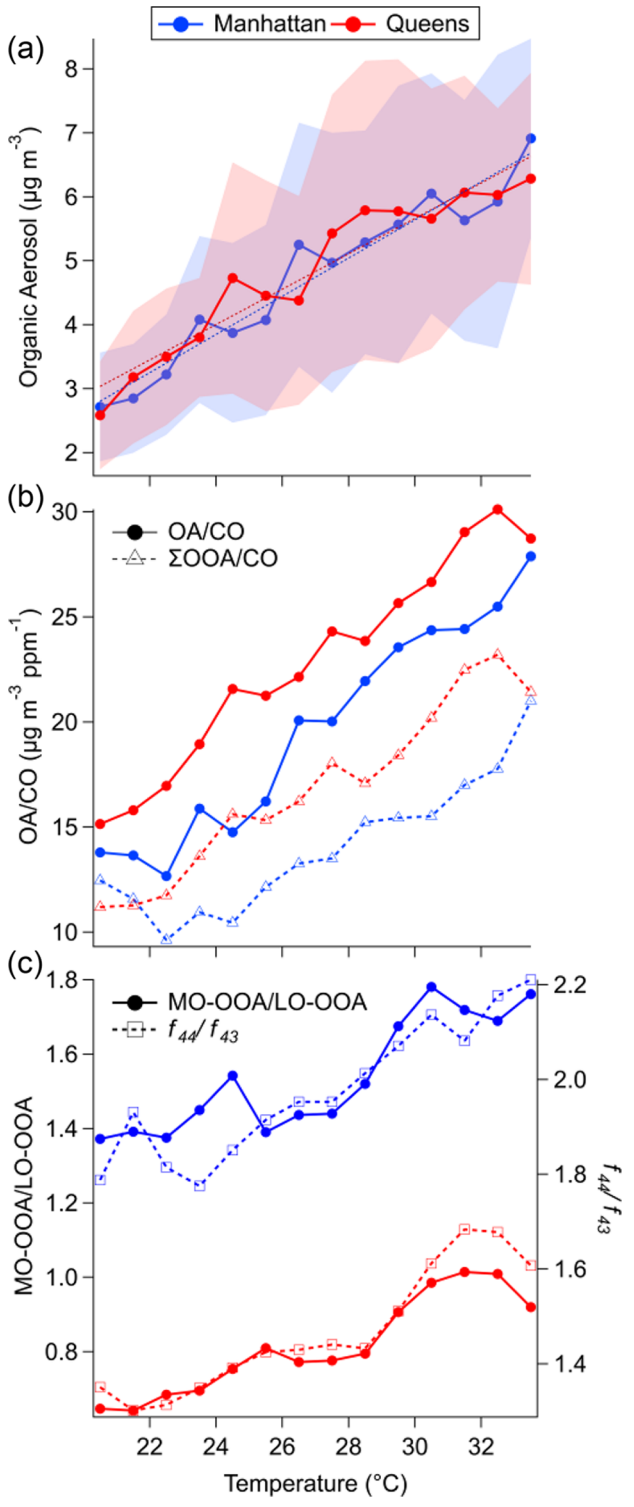

Figure 8. Trends in organic aerosol with temperature in Manhattan and Queens for (a) bulk organic aerosol (OA), (b) dilution-normalized ratios of OA and sum of oxygenated organic aerosol factors (ΣOOA) to carbon monoxide, and (c) ratio of the more oxidized oxygenated organic aerosol (MO-OOA) to less oxidized oxygenated organic aerosol (LO-OOA), shown with f_{44}/f_{43} for comparison. Markers represent mean values of all summer intensive measurements in 1 °C temperature bins with shading in panel (a) representing one standard deviation and shown with linear regression fits (dashed lines, see section 3.4 for values). Coefficients of determination (R^2) for all panels are included in Table S9.

from Los Angeles[55] and the Northeast U.S.[56] This temperature-dependence contributed to significant underprediction of SOA in models/inventories (i.e., CMAQ + VCP) over the LA metropolitan region.[57,58] For comparison, filter measurements of total organic PM fractions across all seasons from 2016–2020 exhibited a slope of 0.51 ± 0.16 μg m^{-3} °C^{-1} (daily averages) for NYC sites.[56] The dilution-normalized ratio of OA/CO had a similar positive correlation with ambient temperature (Manhattan: 1.19 ± 0.08; Queens: 1.16 ± 0.06 μg m^{-3} ppm^{-1} °C^{-1}; Figure 8b), which reinforces that dilution effects did not drive the observed temperature-dependence of OA across sites.

OA source factor correlations with temperature demonstrated that the observed increase in OA with ambient temperature was driven by SOA (Figure S23). Manhattan and Queens showed average OOA slopes of 0.18 ± 0.02 and 0.23 ± 0.02 μg m^{-3} °C^{-1}, respectively (Figure S24), with dilution-normalized OOA/CO slopes of 0.69 ± 0.10 and 0.94 ± 0.06 μg m^{-3} ppm^{-1} °C^{-1}, respectively (Figure 8b). While both LO-OOA and MO-OOA were strongly dependent on temperature, the influence of temperature was more pronounced for MO-OOA (Figure S23a,b). MO-OOA accounted for an increasingly large fraction of OOA with increasing temperatures (Figure 8c). This was evident in both the ratios of MO-OOA/LO-OOA and the ratios of f_{44}/f_{43}, which were similar between sites (Figure 8c); Manhattan and Queens exhibited average MO-OOA/LO-OOA slopes of 0.033 ± 0.005 °C^{-1} and 0.029 ± 0.003 °C^{-1}, and average f_{44}/f_{43} slopes of 0.032 ± 0.004 °C^{-1} and 0.029 ± 0.003 °C^{-1}, respectively. Contrastingly, HOA did not exhibit an increase with temperature (Figure S23d), and interestingly, COA exhibited a moderate increase with temperature that could potentially be associated with outdoor human activity patterns (Figure S23c).

OA concentrations increased with temperature despite any offsetting effects from enhanced OA partitioning to the gas-phase at higher temperatures. These temperature-driven enhancements in summertime PM are very likely influenced by a combination of temperature-dependent VOC-SVOC emissions, comprised of an uncertain mix of both biogenic and anthropogenic VOCs, as well as chemical processing occurring across local and regional scales.[12,55,56] While biogenic VOCs are known to be highly temperature-dependent,[59] there is increasing evidence for temperature-dependent anthropogenic VOCs as well. This includes in NYC where Cao et al.[12] observed distinct enhancements in some anthropogenic VOC concentrations with temperature, which together with urban biogenic/biological sources led to increased OH reactivity in densely-populated Manhattan with unseasonably-high spring-time temperatures. Similar temperature dependence in the total VOC-related OH reactivity was also observed from the diverse mix of biogenic and anthropogenic sources in California's Central Valley.[60] Although a relatively more uncertain area that warrants further research, chemical processes leading to SOA formation can also be temperature-sensitive (e.g., HO_x [OH + HO_2] production),[61] with potential evidence for increased photochemistry observed in both Queens and the Bronx with trends towards lower NO_x/NO_y ratios at higher temperatures (Figure S25).

Meteorology and transport can also play important roles in high-temperature pollution events and background OA composition coming to NYC, with the influence of transport on aerosol composition previously shown for the Queens site

https://doi.org/10.1021/acsestair.3c00037
ACS EST Air 2024, 1, 113–128

in 2009.[19] However, a comparison of wind distributions, speeds, and back-trajectories above and below the average daytime temperature (28.5°C) during the measurement intensive suggests that dilution, transport, and meteorology cannot explain the observed OA dependence (Figures S20 and S26−S30). For example, warmer conditions did not result in stagnation; instead, wind speeds similar to or greater than average were observed at both sites (Figures S27 and S28). Additionally, while backward trajectories coming from the Atlantic Ocean coincided more often with relatively cooler ambient temperatures than other trajectories (Figure S20), OA still exhibited a similar positive correlation with temperature during the subset of measurements where air masses only came from the Atlantic Ocean (Figure S26). This demonstrates that the observed temperature dependence of OA was not driven by influences from potentially cleaner background concentrations aligned with cooler conditions. This overall evaluation of meteorological differences compliments the dilution-normalized analyses of PM's temperature trends as CO did not consistently increase with ambient temperature at either site (Figure S31), and BC's minor temperature trends (Figure S22) further provide a potential upper limit for dilution effects. Together, these results for NYC suggest that stagnation did not drive the observed temperature-dependence of OA across both sites. Still, meteorology is inherently intertwined with temperature and is an influential, location-dependent factor in air quality, so future studies in other domains or seasons should examine the influence of meteorology, especially under a changing climate.

The temperature-dependence of NYC's OA composition, and overall air quality, was particularly pronounced during a major heatwave event that took place from July 20−24 (Figure 3a,c). While there were several periods during the measurement intensive with above average temperatures, this was the only period that qualified as a heatwave according to the common regional definition in the northeastern U.S. as a period of three or more consecutive days with a daily maximum temperature greater than 32.2°C (90 °F; e.g., NYC Office of Emergency Management[62]). During this heatwave event, windspeeds similar to study averages were observed (Figure S7), and absolute PM concentrations were enhanced (compared to study averages) by 3.9 $\mu g\ m^{-3}$ (62%) and 2.4 $\mu g\ m^{-3}$ (41%), while OA concentrations were enhanced by 2.7 $\mu g\ m^{-3}$ (60%) and 1.8 $\mu g\ m^{-3}$ (42%) in Queens and Manhattan, respectively. These heatwave enhancements in OA concentrations were also evident when normalized by CO to account for dilution effects, with enhancements of 33−34% (Figure S32 and Tables S8 and S9). Similar to the general temperature-dependent relationships (Figures 7 and S21−S23), enhancements in total OOA concentrations as well as dilution-normalized OOA concentrations were pronounced during the heatwave event (July 20−24), indicating greater SOA formation influencing the city (Figure S32 and Tables S8 and S9). Primary-like factors including COA and HOA showed comparatively smaller heatwave enhancements, with minor COA enhancements potentially influenced by increases in outdoor human activity as this heatwave spanned a weekend that had major COA spikes on Friday−Sunday (Figure S32 and Tables S8 and S9). While PM composition was dominated by organics, the inorganics, excluding chloride, showed greater heatwave enhancements in Queens compared to Manhattan, including when normalized by CO (Tables S8 and S9). This was especially pronounced for sulfate (and associated ammonium), which showed a strong temperature dependence across the entire measurement intensive (Figure S22) and in prior work.[56]

3.5. Implications for Air Quality in Metropolitan NYC and Downwind Areas. NYC and other U.S. urban areas have achieved sizable improvements in air quality over the past several decades due to concerted efforts to control emissions of primary pollutants and reactive precursors to secondary gas- and particle-phase pollutants; however, comparatively limited gains in $PM_{2.5}$ concentrations have been made over recent years (Figure 1a). Summertime inorganic aerosol concentrations have substantially declined over the past two decades due to successful control measures (e.g., SO_2 emissions reductions, Figure 1a), such that summertime PM is now over 80% organic. This trend has recently been observed in other major U.S. cities (e.g., greater Los Angeles, Atlanta).[37,63] OA concentrations in NYC have remained persistently high since 2009 (Figure 4b,c) and are increasingly due to secondary production. SOA was the dominant component at both the Manhattan and Queens sites, representing ∼53% of the total aerosol observed via ACSM in summer 2022. However, despite the relative proximity of the two sites (14 km), significantly more aged OOA was observed at the Manhattan site compared to that at Queens, given variations in upwind influences. While the observed LO-OOA was generally more attributed to SOA production in or near the city, MO-OOA enhancements suggest greater contributions from upwind regional SOA production (and LO-OOA aging). Despite the density of anthropogenic activity in NYC, these observed SOA enhancements have uncertain contributions from a diverse mix of anthropogenic, biogenic, and marine sources within and outside the city, which necessitates further research. The source apportionment results (Figure 5), along with scatterplots of OA source factors (Figure 6), highlight the spatiotemporal variability in aerosol source contributions that show little correlation between COA and HOA with considerable variability in LO-OOA. Yet, similar general trends in overall aerosol component concentrations (Figures 3 and S10) highlight the effect of regional meteorology and background conditions.

The observed temperature-dependence of OA at both sites warrants greater attention to temperature-sensitive emissions and subsequent chemical processing and highlights the importance of changing climate conditions on summertime air quality in NYC. Elevated temperatures, including but not limited to extreme heat events, are likely to play an increasingly critical role in both the magnitude and composition of PM in NYC and similar cities along the Atlantic coast, with a projected NY statewide temperature increase of 1.67 °C by 2080.[56,57,64] In the NYC region and elsewhere, the feedbacks between climate change and air quality, including temperature-dependent OA enhancements, are inherently complex. These feedbacks are influenced by a diverse mix of temperature-sensitive anthropogenic and biogenic sources, as well as physical/chemical processes, all of which occur across a range of local, regional, and even long-distance scales (e.g., wildfire emissions transport).[65] Future work will benefit from the coupled analysis of chemically detailed gas/aerosol measurements, emissions inventories, and chemical-transport models to deconvolve the varying influences of emissions, chemistry, local meteorology, and transport. These climate-related changes may be coupled with policy-related emissions

https://doi.org/10.1021/acsestair.3c00037
ACS EST Air 2024, 1, 113−128

reductions that could affect the mix of sources of organic and inorganic aerosol precursors or chemical conditions regulating aerosol production. This includes reductions in SO_2/SO_4^{2-} that could impact aerosol oxidation pathways or NO_x emissions reductions that may move away from "high-NO_x" oxidation regimes and increase SOA yields, but may also change RO_2 radical reaction pathways.[66−69]

Together with the expected greater detrimental health effects of SOA[2] and the influence of increased aging on cellular toxicity,[70−73] the predominance of OA amidst summertime $PM_{2.5}$ averages of 8.0−11.4 $\mu g\ m^{-3}$ (2020−2022; Figure S2) and stagnant progress on OA concentrations poses questions for air quality policy. This is especially challenging given the strong influence of temperature on OA concentrations, composition, and age (Figure 8). Notably, while significant sources of biomass burning OA were not measured during this campaign, this is likely to change in the future with warming summertime temperatures and increasingly frequent heatwave events due to a changing climate. Combined, these processes will influence the atmospheric SOA burden and its health impacts in NYC and downwind areas.

■ ASSOCIATED CONTENT

Supporting Information

The Supporting Information is available free of charge at https://pubs.acs.org/doi/10.1021/acsestair.3c00037.

Additional details and figures/tables on ACSM calibrations, hardware, data processing, data validation, and instrument uptimes; Description of PMF analysis method, diagnostic plots, and source factor validation; Long-term trends in $PM_{2.5}$ summertime concentrations throughout NYC and associated map of included sites; Additional concentration wind roses and diurnal profiles of various particle- and gas-phase species; HYSPLIT backward air mass trajectories; Additional temperature dependence plots; Heatwave enhancements in pollutant concentrations (PDF)

■ AUTHOR INFORMATION

Corresponding Author

Drew R. Gentner − *Department of Chemical and Environmental Engineering, Yale University, New Haven, Connecticut 06511, United States*; Email: drew.gentner@yale.edu

Authors

Tori Hass-Mitchell − *Department of Chemical and Environmental Engineering, Yale University, New Haven, Connecticut 06511, United States;* orcid.org/0000-0002-8588-0769

Taekyu Joo − *Department of Chemical and Environmental Engineering, Yale University, New Haven, Connecticut 06511, United States;* orcid.org/0000-0002-8252-4232

Mitchell Rogers − *Department of Chemical and Environmental Engineering, Yale University, New Haven, Connecticut 06511, United States*

Benjamin A. Nault − *Center for Aerosol and Cloud Chemistry, Aerodyne Research Inc., Billerica, Massachusetts 01821, United States;* Present Address: Department of Environmental Health and Engineering, Johns Hopkins University, Baltimore, MD 21205, U.S.A; orcid.org/0000-0001-9464-4787

Catelynn Soong − *Department of Chemical and Environmental Engineering, Yale University, New Haven, Connecticut 06511, United States*

Mia Tran − *Department of Chemical and Environmental Engineering, Yale University, New Haven, Connecticut 06511, United States*

Minguk Seo − *Department of Chemical and Environmental Engineering, Yale University, New Haven, Connecticut 06511, United States*

Jo Ellen Machesky − *Department of Chemical and Environmental Engineering, Yale University, New Haven, Connecticut 06511, United States*

Manjula Canagaratna − *Center for Aerosol and Cloud Chemistry, Aerodyne Research Inc., Billerica, Massachusetts 01821, United States*

Joseph Roscioli − *Center for Aerosol and Cloud Chemistry, Aerodyne Research Inc., Billerica, Massachusetts 01821, United States*

Megan S. Claflin − *Center for Aerosol and Cloud Chemistry, Aerodyne Research Inc., Billerica, Massachusetts 01821, United States;* orcid.org/0000-0003-0878-8712

Brian M. Lerner − *Center for Aerosol and Cloud Chemistry, Aerodyne Research Inc., Billerica, Massachusetts 01821, United States*

Daniel C. Blomdahl − *Department of Civil, Architectural, and Environmental Engineering, University of Texas at Austin, Austin, Texas 78712, United States;* orcid.org/0000-0002-2004-0937

Pawel K. Misztal − *Department of Civil, Architectural, and Environmental Engineering, University of Texas at Austin, Austin, Texas 78712, United States;* orcid.org/0000-0003-1060-1750

Nga L. Ng − *School of Chemical and Biomolecular Engineering, Georgia Institute of Technology, Atlanta, Georgia 30332, United States; School of Earth and Atmospheric Sciences and School of Civil and Environmental Engineering, Georgia Institute of Technology, Atlanta, Georgia 30332, United States;* orcid.org/0000-0001-8460-4765

Ann M. Dillner − *Air Quality Research Center, University of California Davis, Davis, California 95618, United States*

Roya Bahreini − *Department of Environmental Sciences, University of California, Riverside, California 92521, United States*

Armistead Russell − *School of Civil and Environmental Engineering, Georgia Institute of Technology, Atlanta, Georgia 30332, United States;* orcid.org/0000-0003-2027-8870

Jordan E. Krechmer − *Center for Aerosol and Cloud Chemistry, Aerodyne Research Inc., Billerica, Massachusetts 01821, United States;* Present Address: Bruker Daltonics, Billerica, MA 01821, U.S.A.

Andrew Lambe − *Center for Aerosol and Cloud Chemistry, Aerodyne Research Inc., Billerica, Massachusetts 01821, United States;* orcid.org/0000-0003-3031-701X

Complete contact information is available at: https://pubs.acs.org/10.1021/acsestair.3c00037

Author Contributions

D.R.G., A.L., J.E.K., N.L.N., A.M.D., R.B., and A.R. conceived the study and/or the broader NYC-METS and ASCENT Projects. T.H.M. led data analysis and writing with support

https://doi.org/10.1021/acsestair.3c00037
ACS EST Air 2024, 1, 113−128

from T.J., M.R., B.A.N., C.S., and D.R.G., with contributions and review from co-authors. T.H.M. and T.J. performed ACSM calibrations and data collection in Queens, while B.A.N., T.J., and T.H.M. did so in Manhattan. B.A.N. and M.C. provided support with source apportionment analyses. M.R. led the temperature-dependent aerosol analysis. J.E.M., A.L., and J.K. led collection and processing of HR-TOF-CIMS data. J.E.K. and M.T. led data collection and processing of Vocus PTR-TOF-MS data. M.S.C., B.M.L., D.C.B., and P.K.M led data collection and processing of in-situ GC-TOF data. M.R., M.T., J.E.M., M.S., and J.R. led data collection and processing of other supporting data in Manhattan, including BC, CO, O_3, NO_x, SO_2, and meteorological data.

■ ACKNOWLEDGMENTS

We thank the National Oceanic and Atmospheric Administration (NOAA) for funding this research (NA20OAR4310304, NA20OAR4310305, NA21OAR4310140, NA21OAR4310141) under the NYC-METS Project as part of the broader AGES campaign, and NSF for supporting the ASCENT network (AGS-2131914). T.H.M. and C.S. acknowledge support from the NSF INTERN program and NSF Atmospheric Chemistry (AGS-2131084). D.R.G., T.H.M., and T.J. also thank the New York State Energy Research and Development Authority (NYSERDA) for supporting this research (Agreement No. 183866). D.C.B. acknowledges support from the National Science Foundation Graduate Research Fellowship under Grant No. DGE 2137420. Any opinions expressed in this article do not necessarily reflect those of NYSERDA or the State of New York. We thank the City University of New York, specifically Ricardo Toledo-Crow, for hosting sampling at their Advanced Science Research Center (CUNY ASRC). We also thank the New York State Department of Environmental Conservation (NYSDEC) as well as Queens College for hosting sampling at their Queens College monitoring site and providing supporting data from the Queens and Bronx sites. The detailed meteorology data from the Queens site was made possible by the New York State (NYS) Mesonet. Original funding for the NYS Mesonet was provided by Federal Emergency Management Agency Grant FEMA-4085-DR-NY, with the continued support of the NYS Division of Homeland Security and Emergency Services; the State of New York; the Research Foundation for the State University of New York (SUNY); the University at Albany; the Atmospheric Sciences Research Center (ASRC) at the University at Albany; and the Department of Atmospheric and Environmental Sciences (DAES) at the University at Albany.

■ REFERENCES

(1) Landrigan, P. J.; Fuller, R.; Acosta, N. J. R.; Adeyi, O.; Arnold, R.; Basu, N.; Baldé, A. B.; Bertollini, R.; Bose-O'Reilly, S.; Boufford, J. I.; Breysse, P. N.; Chiles, T.; Mahidol, C.; Coll-Seck, A. M.; Cropper, M. L.; Fobil, J.; Fuster, V.; Greenstone, M.; Haines, A.; Hanrahan, D.; Hunter, D.; Khare, M.; Krupnick, A.; Lanphear, B.; Lohani, B.; Martin, K.; Mathiasen, K. V.; McTeer, M. A.; Murray, C. J. L.; Ndahimananjara, J. D.; Perera, F.; Potočnik, J.; Preker, A. S.; Ramesh, J.; Rockström, J.; Salinas, C.; Samson, L. D.; Sandilya, K.; Sly, P. D.; Smith, K. R.; Steiner, A.; Stewart, R. B.; Suk, W. A.; van Schayck, O. C. P.; Yadama, G. N.; Yumkella, K.; Zhong, M. The Lancet Commission on Pollution and Health. *Lancet* **2018**, *391* (10119), 462−512.

(2) Pye, H. O. T.; Ward-Caviness, C. K.; Murphy, B. N.; Appel, K. W.; Seltzer, K. M. Secondary Organic Aerosol Association with Cardiorespiratory Disease Mortality in the United States. *Nat. Commun.* **2021**, *12* (1), 7215.

(3) Zhang, Q.; Jimenez, J. L.; Canagaratna, M. R.; Allan, J. D.; Coe, H.; Ulbrich, I.; Alfarra, M. R.; Takami, A.; Middlebrook, A. M.; Sun, Y. L.; Dzepina, K.; Dunlea, E.; Docherty, K.; DeCarlo, P. F.; Salcedo, D.; Onasch, T.; Jayne, J. T.; Miyoshi, T.; Shimono, A.; Hatakeyama, S.; Takegawa, N.; Kondo, Y.; Schneider, J.; Drewnick, F.; Borrmann, S.; Weimer, S.; Demerjian, K.; Williams, P.; Bower, K.; Bahreini, R.; Cottrell, L.; Griffin, R. J.; Rautiainen, J.; Sun, J. Y.; Zhang, Y. M.; Worsnop, D. R. Ubiquity and Dominance of Oxygenated Species in Organic Aerosols in Anthropogenically-Influenced Northern Hemisphere Midlatitudes. *Geophys. Res. Lett.* **2007**, *34*, L13801.

(4) Hoffmann, B.; Boogaard, H.; de Nazelle, A.; Andersen, Z. J.; Abramson, M.; Brauer, M.; Brunekreef, B.; Forastiere, F.; Huang, W.; Kan, H.; Kaufman, J. D.; Katsouyanni, K.; Krzyzanowski, M.; Kuenzli, N.; Laden, F.; Nieuwenhuijsen, M.; Mustapha, A.; Powell, P.; Rice, M.; Roca-Barceló, A.; Roscoe, C. J.; Soares, A.; Straif, K.; Thurston, G. WHO Air Quality Guidelines 2021-Aiming for Healthier Air for All: A Joint Statement by Medical, Public Health, Scientific Societies and Patient Representative Organisations. *Int. J. Public Health* **2021**, *66*, 1604465.

(5) Weichenthal, S.; Pinault, L.; Christidis, T.; Burnett, R. T.; Brook, J. R.; Chu, Y.; Crouse, D. L.; Erickson, A. C.; Hystad, P.; Li, C.; Martin, R. V.; Meng, J.; Pappin, A. J.; Tjepkema, M.; van Donkelaar, A.; Weagle, C. L.; Brauer, M. How Low Can You Go? Air Pollution Affects Mortality at Very Low Levels. *Sci. Adv.* **2022**, *8* (39), No. eabo3381.

(6) Robinson, A. L.; Donahue, N. M.; Shrivastava, M. K.; Weitkamp, E. A.; Sage, A. M.; Grieshop, A. P.; Lane, T. E.; Pierce, J. R.; Pandis, S. N. Rethinking Organic Aerosols: Semivolatile Emissions and Photochemical Aging. *Science* **2007**, *315* (5816), 1259−1262.

(7) Ervens, B.; Turpin, B. J.; Weber, R. J. Secondary Organic Aerosol Formation in Cloud Droplets and Aqueous Particles (aqSOA): A Review of Laboratory, Field and Model Studies. *Atmospheric Chem. Phys.* **2011**, *11* (21), 11069−11102.

(8) McNeill, V. F. Aqueous Organic Chemistry in the Atmosphere: Sources and Chemical Processing of Organic Aerosols. *Environ. Sci. Technol.* **2015**, *49* (3), 1237−1244.

(9) Khare, P.; Gentner, D. R. Considering the Future of Anthropogenic Gas-Phase Organic Compound Emissions and the Increasing Influence of Non-Combustion Sources on Urban Air Quality. *Atmospheric Chem. Phys.* **2018**, *18* (8), 5391−5413.

(10) McDonald, B. C.; de Gouw, J. A.; Gilman, J. B.; Jathar, S. H.; Akherati, A.; Cappa, C. D.; Jimenez, J. L.; Lee-Taylor, J.; Hayes, P. L.; McKeen, S. A.; Cui, Y. Y.; Kim, S.-W.; Gentner, D. R.; Isaacman-VanWertz, G.; Goldstein, A. H.; Harley, R. A.; Frost, G. J.; Roberts, J. M.; Ryerson, T. B.; Trainer, M. Volatile Chemical Products Emerging as Largest Petrochemical Source of Urban Organic Emissions. *Science* **2018**, *359* (6377), 760−764.

(11) Gkatzelis, G. I.; Coggon, M. M.; McDonald, B. C.; Peischl, J.; Gilman, J. B.; Aikin, K. C.; Robinson, M. A.; Canonaco, F.; Prevot, A. S. H.; Trainer, M.; Warneke, C. Observations Confirm That Volatile Chemical Products Are a Major Source of Petrochemical Emissions in U.S. Cities. *Environ. Sci. Technol.* **2021**, *55* (8), 4332−4343.

(12) Cao, C.; Gentner, D. R.; Commane, R.; Toledo-Crow, R.; Schiferl, L. D.; Mak, J. E. Policy-Related Gains in Urban Air Quality May Be Offset by Increased Emissions in a Warming Climate. *Environ. Sci. Technol.* **2023**, *57*, 9683−9692.

(13) U.S. EPA. NAAQS Table. https://www.epa.gov/criteria-air-pollutants/naaqs-table (accessed 2023-07-06).

(14) Canagaratna, M. r.; Jayne, J. t.; Jimenez, J. l.; Allan, J. d.; Alfarra, M. r.; Zhang, Q.; Onasch, T. b.; Drewnick, F.; Coe, H.; Middlebrook, A.; Delia, A.; Williams, L. r.; Trimborn, A. m.; Northway, M. j.; DeCarlo, P. f.; Kolb, C. e.; Davidovits, P.; Worsnop, D. r. Chemical and Microphysical Characterization of Ambient Aerosols with the Aerodyne Aerosol Mass Spectrometer. *Mass Spectrom. Rev.* **2007**, *26* (2), 185−222.

(15) Ulbrich, I. M.; Canagaratna, M. R.; Zhang, Q.; Worsnop, D. R.; Jimenez, J. L. Interpretation of Organic Components from Positive

https://doi.org/10.1021/acsestair.3c00037
ACS EST Air 2024, 1, 113−128

Matrix Factorization of Aerosol Mass Spectrometric Data. *Atmospheric Chem. Phys.* **2009**, *9* (9), 2891−2918.
(16) Drewnick, F.; Jayne, J. T.; Canagaratna, M.; Worsnop, D. R.; Demerjian, K. L. Measurement of Ambient Aerosol Composition During the PMTACS-NY 2001 Using an Aerosol Mass Spectrometer. Part II: Chemically Speciated Mass Distributions Special Issue of Aerosol Science and Technology on Findings from the Fine Particulate Matter Supersites Program. *Aerosol Sci. Technol.* **2004**, *38* (sup1), 104−117.
(17) Drewnick, F.; Schwab, J. J.; Jayne, J. T.; Canagaratna, M.; Worsnop, D. R.; Demerjian, K. L. Measurement of Ambient Aerosol Composition During the PMTACS-NY 2001 Using an Aerosol Mass Spectrometer. Part I: Mass Concentrations Special Issue of *Aerosol Science and Technology* on Findings from the Fine Particulate Matter Supersites Program. *Aerosol Sci. Technol.* **2004**, *38* (sup1), 92−103.
(18) Li, Z.; Hopke, P. K.; Husain, L.; Qureshi, S.; Dutkiewicz, V. A.; Schwab, J. J.; Drewnick, F.; Demerjian, K. L. Sources of Fine Particle Composition in New York City. *Atmos. Environ.* **2004**, *38* (38), 6521−6529.
(19) Sun, Y.-L.; Zhang, Q.; Schwab, J. J.; Demerjian, K. L.; Chen, W.-N.; Bae, M.-S.; Hung, H.-M.; Hogrefe, O.; Frank, B.; Rattigan, O. V.; Lin, Y.-C. Characterization of the Sources and Processes of Organic and Inorganic Aerosols in New York City with a High-Resolution Time-of-Flight Aerosol Mass Apectrometer. *Atmospheric Chem. Phys.* **2011**, *11* (4), 1581−1602.
(20) Schroder, J. C.; Campuzano-Jost, P.; Day, D. A.; Shah, V.; Larson, K.; Sommers, J. M.; Sullivan, A. P.; Campos, T.; Reeves, J. M.; Hills, A.; Hornbrook, R. S.; Blake, N. J.; Scheuer, E.; Guo, H.; Fibiger, D. L.; McDuffie, E. E.; Hayes, P. L.; Weber, R. J.; Dibb, J. E.; Apel, E. C.; Jaeglé, L.; Brown, S. S.; Thornton, J. A.; Jimenez, J. L. Sources and Secondary Production of Organic Aerosols in the Northeastern United States during WINTER. *J. Geophys. Res. Atmospheres* **2018**, *123* (14), 7771−7796.
(21) Shah, V.; Jaeglé, L.; Jimenez, J. L.; Schroder, J. C.; Campuzano-Jost, P.; Campos, T. L.; Reeves, J. M.; Stell, M.; Brown, S. S.; Lee, B. H.; Lopez-Hilfiker, F. D.; Thornton, J. A. Widespread Pollution From Secondary Sources of Organic Aerosols During Winter in the Northeastern United States. *Geophys. Res. Lett.* **2019**, *46* (5), 2974−2983.
(22) Coggon, M. M.; Gkatzelis, G. I.; McDonald, B. C.; Gilman, J. B.; Schwantes, R. H.; Abuhassan, N.; Aikin, K. C.; Arend, M. F.; Berkoff, T. A.; Brown, S. S.; Campos, T. L.; Dickerson, R. R.; Gronoff, G.; Hurley, J. F.; Isaacman-VanWertz, G.; Koss, A. R.; Li, M.; McKeen, S. A.; Moshary, F.; Peischl, J.; Pospisilova, V.; Ren, X.; Wilson, A.; Wu, Y.; Trainer, M.; Warneke, C. Volatile Chemical Product Emissions Enhance Ozone and Modulate Urban Chemistry. *Proc. Natl. Acad. Sci. U. S. A.* **2021**, *118* (32), No. e2026653118.
(23) Khare, P.; Krechmer, J. E.; Machesky, J. E.; Hass-Mitchell, T.; Cao, C.; Wang, J.; Majluf, F.; Lopez-Hilfiker, F.; Malek, S.; Wang, W.; Seltzer, K.; Pye, H. O. T.; Commane, R.; McDonald, B. C.; Toledo-Crow, R.; Mak, J. E.; Gentner, D. R. Ammonium-Adduct Chemical Ionization to Investigate Anthropogenic Oxygenated Gas-Phase Organic Compounds in Urban Air. *Atmospheric Chem. Phys. Discuss.* **2022**, *22* (21), 14377−14399.
(24) Masiol, M.; Squizzato, S.; Rich, D. Q.; Hopke, P. K. Long-Term Trends (2005-2016) of Source Apportioned PM2.5 across New York State. *Atmos. Environ.* **2019**, *201*, 110−120.
(25) Pitiranggon, M.; Johnson, S.; Haney, J.; Eisl, H.; Ito, K. Long-Term Trends in Local and Transported PM2.5 Pollution in New York City. *Atmos. Environ.* **2021**, *248*, 118238.
(26) Rattigan, O. V.; Civerolo, K. L.; Felton, H. D.; Schwab, J. J.; Demerjian, K. L. Long Term Trends in New York: PM2.5 Mass and Particle Components. *Aerosol Air Qual. Res.* **2016**, *16* (5), 1191−1205.
(27) Chen, Y.; Rich, D. Q.; Hopke, P. K. Long-Term PM2.5 Source Analyses in New York City from the Perspective of Dispersion Normalized PMF. *Atmos. Environ.* **2022**, *272*, 118949.
(28) Nault, B. A.; Jo, D. S.; McDonald, B. C.; Campuzano-Jost, P.; Day, D. A.; Hu, W.; Schroder, J. C.; Allan, J.; Blake, D. R.; Canagaratna, M. R.; Coe, H.; Coggon, M. M.; DeCarlo, P. F.; Diskin, G. S.; Dunmore, R.; Flocke, F.; Fried, A.; Gilman, J. B.; Gkatzelis, G.; Hamilton, J. F.; Hanisco, T. F.; Hayes, P. L.; Henze, D. K.; Hodzic, A.; Hopkins, J.; Hu, M.; Huey, L. G.; Jobson, B. T.; Kuster, W. C.; Lewis, A.; Li, M.; Liao, J.; Nawaz, M. O.; Pollack, I. B.; Peischl, J.; Rappenglück, B.; Reeves, C. E.; Richter, D.; Roberts, J. M.; Ryerson, T. B.; Shao, M.; Sommers, J. M.; Walega, J.; Warneke, C.; Weibring, P.; Wolfe, G. M.; Young, D. E.; Yuan, B.; Zhang, Q.; de Gouw, J. A.; Jimenez, J. L. Secondary Organic Aerosols from Anthropogenic Volatile Organic Compounds Contribute Substantially to Air Pollution Mortality. *Atmospheric Chem. Phys.* **2021**, *21* (14), 11201−11224.
(29) Warneke, C.; Schwantes, R. H.; Veres, P. R.; Rollins, A.; Baidar, S.; Brewer, W. A.; Senff, C.; Langford, A.; Aikin, K. C.; Frost, G. J.; Fahey, D.; Judd, L. M.; Lefer, B. L.; Pierce, B.; Kondragunta, S.; Stockwell, C.; Gentner, D. R.; Lambe, A. T.; Millet, D. B.; Farmer, D. K.; Ng, N. L.; Kaiser, J.; Young, C.; Mak, J. E.; Wolfe, G. M.; Sullivan, J.; Mueller, K.; Karion, A.; Valin, L.; Witte, M.; Russell, L. M.; Ren, X.; Dickerson, R. R.; DeCarlo, P. F.; McDonald, B. C.; Brown, S. S. The AEROMMA 2023 Experiment (Atmospheric Emissions and Reactions Observed from Megacities to Marine Areas) [White Paper], 2022. https://csl.noaa.gov/projects/aeromma/whitepaper.pdf.
(30) Ng, N. L.; Herndon, S. C.; Trimborn, A.; Canagaratna, M. R.; Croteau, P. L.; Onasch, T. B.; Sueper, D.; Worsnop, D. R.; Zhang, Q.; Sun, Y. L.; Jayne, J. T. An Aerosol Chemical Speciation Monitor (ACSM) for Routine Monitoring of the Composition and Mass Concentrations of Ambient Aerosol. *Aerosol Sci. Technol.* **2011**, *45* (7), 780−794.
(31) Fröhlich, R.; Cubison, M. J.; Slowik, J. G.; Bukowiecki, N.; Prévôt, A. S. H.; Baltensperger, U.; Schneider, J.; Kimmel, J. R.; Gonin, M.; Rohner, U.; Worsnop, D. R.; Jayne, J. T. The ToF-ACSM: A Portable Aerosol Chemical Speciation Monitor with TOFMS Detection. *Atmospheric Meas. Technol.* **2013**, *6* (11), 3225−3241.
(32) Ng, N. L.; Canagaratna, M. R.; Jimenez, J. L.; Zhang, Q.; Ulbrich, I. M.; Worsnop, D. R. Real-Time Methods for Estimating Organic Component Mass Concentrations from Aerosol Mass Spectrometer Data. *Environ. Sci. Technol.* **2011**, *45* (3), 910−916.
(33) Timonen, H.; Cubison, M.; Aurela, M.; Brus, D.; Lihavainen, H.; Hillamo, R.; Canagaratna, M.; Nekat, B.; Weller, R.; Worsnop, D.; Saarikoski, S. Applications and Limitations of Constrained High-Resolution Peak Fitting on Low Resolving Power Mass Spectra from the ToF-ACSM. *Atmospheric Meas. Technol.* **2016**, *9* (7), 3263−3281.
(34) Xu, W.; Croteau, P.; Williams, L.; Canagaratna, M.; Onasch, T.; Cross, E.; Zhang, X.; Robinson, W.; Worsnop, D.; Jayne, J. Laboratory Characterization of an Aerosol Chemical Speciation Monitor with PM2.5 Measurement Capability. *Aerosol Sci. Technol.* **2017**, *51* (1), 69−83.
(35) Hu, W.; Campuzano-Jost, P.; Day, D. A.; Croteau, P.; Canagaratna, M. R.; Jayne, J. T.; Worsnop, D. R.; Jimenez, J. L. Evaluation of the New Capture Vaporizer for Aerosol Mass Spectrometers (AMS) through Field Studies of Inorganic Species. *Aerosol Sci. Technol.* **2017**, *51* (6), 735−754.
(36) Hu, W.; Campuzano-Jost, P.; Day, D. A.; Nault, B. A.; Park, T.; Lee, T.; Pajunoja, A.; Virtanen, A.; Croteau, P.; Canagaratna, M. R.; Jayne, J. T.; Worsnop, D. R.; Jimenez, J. L. Ambient Quantification and Size Distributions for Organic Aerosol in Aerosol Mass Spectrometers with the New Capture Vaporizer. *ACS Earth Space Chem.* **2020**, *4* (5), 676−689.
(37) Joo, T.; Chen, Y.; Xu, W.; Croteau, P.; Canagaratna, M. R.; Gao, D.; Guo, H.; Saavedra, G.; Kim, S. S.; Sun, Y.; Weber, R.; Jayne, J.; Ng, N. L. Evaluation of a New Aerosol Chemical Speciation Monitor (ACSM) System at an Urban Site in Atlanta, GA: The Use of Capture Vaporizer and PM2.5 Inlet. *ACS Earth Space Chem.* **2021**, *5* (10), 2565−2576.
(38) Kimmel, J. R.; Farmer, D. K.; Cubison, M. J.; Sueper, D.; Tanner, C.; Nemitz, E.; Worsnop, D. R.; Gonin, M.; Jimenez, J. L. Real-Time Aerosol Mass Spectrometry with Millisecond Resolution. *Int. J. Mass Spectrom.* **2011**, *303* (1), 15−26.

(39) Krechmer, J.; Lopez-Hilfiker, F.; Koss, A.; Hutterli, M.; Stoermer, C.; Deming, B.; Kimmel, J.; Warneke, C.; Holzinger, R.; Jayne, J.; Worsnop, D.; Fuhrer, K.; Gonin, M.; de Gouw, J. Evaluation of a New Reagent-Ion Source and Focusing Ion-Molecule Reactor for Use in Proton-Transfer-Reaction Mass Spectrometry. *Anal. Chem.* **2018**, *90* (20), 12011−12018.
(40) Sekimoto, K.; Li, S.-M.; Yuan, B.; Koss, A.; Coggon, M.; Warneke, C.; de Gouw, J. Calculation of the Sensitivity of Proton-Transfer-Reaction Mass Spectrometry (PTR-MS) for Organic Trace Gases Using Molecular Properties. *Int. J. Mass Spectrom.* **2017**, *421*, 71−94.
(41) Claflin, M. S.; Pagonis, D.; Finewax, Z.; Handschy, A. V.; Day, D. A.; Brown, W. L.; Jayne, J. T.; Worsnop, D. R.; Jimenez, J. L.; Ziemann, P. J.; de Gouw, J.; Lerner, B. M. An in Situ Gas Chromatograph with Automatic Detector Switching between PTR- and EI-TOF-MS: Isomer-Resolved Measurements of Indoor Air. *Atmospheric Meas. Technol.* **2021**, *14* (1), 133−152.
(42) Bertram, T. H.; Kimmel, J. R.; Crisp, T. A.; Ryder, O. S.; Yatavelli, R. L. N.; Thornton, J. A.; Cubison, M. J.; Gonin, M.; Worsnop, D. R. A Field-Deployable, Chemical Ionization Time-of-Flight Mass Spectrometer. *Atmospheric Meas. Technol.* **2011**, *4* (7), 1471−1479.
(43) Lee, B. H.; Lopez-Hilfiker, F. D.; Mohr, C.; Kurtén, T.; Worsnop, D. R.; Thornton, J. A. An Iodide-Adduct High-Resolution Time-of-Flight Chemical-Ionization Mass Spectrometer: Application to Atmospheric Inorganic and Organic Compounds. *Environ. Sci. Technol.* **2014**, *48* (11), 6309−6317.
(44) McManus, J. B.; Zahniser, M. S.; Nelson, D. D.; Shorter, J. H.; Herndon, S. C.; Jervis, D.; Agnese, M.; McGovern, R.; Yacovitch, T. I.; Roscioli, J. R. Recent Progress in Laser-Based Trace Gas Instruments: Performance and Noise Analysis. *Appl. Phys. B* **2015**, *119* (1), 203−218.
(45) Brotzge, J. A.; Wang, J.; Thorncroft, C. D.; Joseph, E.; Bain, N.; Bassill, N.; Farruggio, N.; Freedman, J. M.; Hemker, K.; Johnston, D.; Kane, E.; McKim, S.; Miller, S. D.; Minder, J. R.; Naple, P.; Perez, S.; Schwab, J. J.; Schwab, M. J.; Sicker, J. A Technical Overview of the New York State Mesonet Standard Network. *J. Atmospheric Ocean. Technol.* **2020**, *37* (10), 1827−1845.
(46) De Gouw, J.; Jimenez, J. L. Organic Aerosols in the Earth's Atmosphere. *Environ. Sci. Technol.* **2009**, *43* (20), 7614−7618.
(47) Zhang, Q.; Jimenez, J. L.; Canagaratna, M. R.; Ulbrich, I. M.; Ng, N. L.; Worsnop, D. R.; Sun, Y. Understanding Atmospheric Organic Aerosols via Factor Analysis of Aerosol Mass Spectrometry: A Review. *Anal. Bioanal. Chem.* **2011**, *401* (10), 3045−3067.
(48) Orton, P. M.; McGillis, W. R.; Zappa, C. J. Sea Breeze Forcing of Estuary Turbulence and Air-Water CO2 Exchange. *Geophys. Res. Lett.* **2010**, *37*, L13603.
(49) Frizzola, J. A.; Fisher, E. L. A Series of Sea Breeze Observations in the New York City Area. *J. Appl. Meteorol. Climatol.* **1963**, *2* (6), 722−739.
(50) Jimenez, J. L.; Canagaratna, M. R.; Donahue, N. M.; Prevot, A. S. H.; Zhang, Q.; Kroll, J. H.; DeCarlo, P. F.; Allan, J. D.; Coe, H.; Ng, N. L.; Aiken, A. C.; Docherty, K. S.; Ulbrich, I. M.; Grieshop, A. P.; Robinson, A. L.; Duplissy, J.; Smith, J. D.; Wilson, K. R.; Lanz, V. A.; Hueglin, C.; Sun, Y. L.; Tian, J.; Laaksonen, A.; Raatikainen, T.; Rautiainen, J.; Vaattovaara, P.; Ehn, M.; Kulmala, M.; Tomlinson, J. M.; Collins, D. R.; Cubison, M. J.; Dunlea, J.; Huffman, J. A.; Onasch, T. B.; Alfarra, M. R.; Williams, P. I.; Bower, K.; Kondo, Y.; Schneider, J.; Drewnick, F.; Borrmann, S.; Weimer, S.; Demerjian, K.; Salcedo, D.; Cottrell, L.; Griffin, R.; Takami, A.; Miyoshi, T.; Hatakeyama, S.; Shimono, A.; Sun, J. Y.; Zhang, Y. M.; Dzepina, K.; Kimmel, J. R.; Sueper, D.; Jayne, J. T.; Herndon, S. C.; Trimborn, A. M.; Williams, L. R.; Wood, E. C.; Middlebrook, A. M.; Kolb, C. E.; Baltensperger, U.; Worsnop, D. R. Evolution of Organic Aerosols in the Atmosphere. *Science* **2009**, *326* (5959), 1525−1529.
(51) Chen, G.; Canonaco, F.; Slowik, J. G.; Daellenbach, K. R.; Tobler, A.; Petit, J.-E.; Favez, O.; Stavroulas, I.; Mihalopoulos, N.; Gerasopoulos, E.; El Haddad, I.; Baltensperger, U.; Prévôt, A. S. H. Real-Time Source Apportionment of Organic Aerosols in Three European Cities. *Environ. Sci. Technol.* **2022**, *56* (22), 15290−15297.
(52) Ng, N. L.; Canagaratna, M. R.; Jimenez, J. L.; Chhabra, P. S.; Seinfeld, J. H.; Worsnop, D. R. Changes in Organic Aerosol Composition with Aging Inferred from Aerosol Mass Spectra. *Atmospheric Chem. Phys.* **2011**, *11* (13), 6465−6474.
(53) Williams, B. J.; Goldstein, A. H.; Kreisberg, N. M.; Hering, S. V.; Worsnop, D. R.; Ulbrich, I. M.; Docherty, K. S.; Jimenez, J. L. Major Components of Atmospheric Organic Aerosol in Southern California as Determined by Hourly Measurements of Source Marker Compounds. *Atmospheric Chem. Phys.* **2010**, *10* (23), 11577−11603.
(54) Kim, S.; Machesky, J.; Gentner, D. R.; Presto, A. A. Real-World Observations of Ultrafine Particles and Reduced Nitrogen in Commercial Cooking Organic Aerosol Emissions. *EGUsphere* **2023**, na.
(55) Nussbaumer, C. M.; Cohen, R. C. Impact of OA on the Temperature Dependence of PM 2.5 in the Los Angeles Basin. *Environ. Sci. Technol.* **2021**, *55* (6), 3549−3558.
(56) Vannucci, P. F.; Cohen, R. C. Decadal Trends in the Temperature Dependence of Summertime Urban PM2.5 in the Northeast United States. *ACS Earth Space Chem.* **2022**, *6* (7), 1793−1798.
(57) Pennington, E. A.; Seltzer, K. M.; Murphy, B. N.; Qin, M.; Seinfeld, J. H.; Pye, H. O. T. Modeling Secondary Organic Aerosol Formation from Volatile Chemical Products. *Atmospheric Chem. Phys.* **2021**, *21* (24), 18247−18261.
(58) Liu, Y.; Dong, X.; Emmons, L. K.; Jo, D. S.; Liu, Y.; Shrivastava, M.; Yue, M.; Liang, Y.; Song, Z.; He, X.; Wang, M. Exploring the Factors Controlling the Long-Term Trend (1988-2019) of Surface Organic Aerosols in the Continental United States by Simulations. *J. Geophys. Res. Atmospheres* **2023**, *128* (9), No. e2022JD037935.
(59) Guenther, A. B.; Jiang, X.; Heald, C. L.; Sakulyanontvittaya, T.; Duhl, T.; Emmons, L. K.; Wang, X. The Model of Emissions of Gases and Aerosols from Nature Version 2.1 (MEGAN2.1): An Extended and Updated Framework for Modeling Biogenic Emissions. *Geosci. Model Dev.* **2012**, *5* (6), 1471−1492.
(60) Pusede, S. E.; Gentner, D. R.; Wooldridge, P. J.; Browne, E. C.; Rollins, A. W.; Min, K.-E.; Russell, A. R.; Thomas, J.; Zhang, L.; Brune, W. H.; Henry, S. B.; DiGangi, J. P.; Keutsch, F. N.; Harrold, S. A.; Thornton, J. A.; Beaver, M. R.; St. Clair, J. M.; Wennberg, P. O.; Sanders, J.; Ren, X.; VandenBoer, T. C.; Markovic, M. Z.; Guha, A.; Weber, R.; Goldstein, A. H.; Cohen, R. C. On the Temperature Dependence of Organic Reactivity, Nitrogen Oxides, Ozone Production, and the Impact of Emission Controls in San Joaquin Valley, California. *Atmospheric Chem. Phys.* **2014**, *14* (7), 3373−3395.
(61) Pusede, S. E.; Steiner, A. L.; Cohen, R. C. Temperature and Recent Trends in the Chemistry of Continental Surface Ozone. *Chem. Rev.* **2015**, *115* (10), 3898−3918.
(62) Rosenzweig, C.; Solecki, W. D.; Parshall, L.; Lynn, B.; Cox, J.; Goldberg, R.; Hodges, S.; Gaffin, S.; Slosberg, R. B.; Savio, P.; Dunstan, F.; Watson, M. Mitigating New York City's Heat Island: Integrating Stakeholder Perspectives and Scientific Evaluation. *Bull. Am. Meteorol. Soc.* **2009**, *90* (9), 1297−1312.
(63) Tohidi, R.; Altuwayjiri, A.; Pirhadi, M.; Sioutas, C. Quantifying Ambient Concentrations of Primary and Secondary Organic Aerosol in Central Los Angeles Using an Integrated Approach Coupling Source Apportionment with Regression Analysis. *Atmos. Environ.* **2022**, *268*, 118807.
(64) Climate Change Effects and Impacts - NYS Dept. of Environmental Conservation. https://www.dec.ny.gov/energy/94702.html (accessed 2023−11−08).
(65) Rogers, H. M.; Ditto, J. C.; Gentner, D. R. Evidence for Impacts on Surface-Level Air Quality in the Northeastern US from Long-Distance Transport of Smoke from North American Fires during the Long Island Sound Tropospheric Ozone Study (LISTOS) 2018. *Atmospheric Chem. Phys.* **2020**, *20* (2), 671−682.
(66) Pye, H. O. T.; D'Ambro, E. L.; Lee, B. H.; Schobesberger, S.; Takeuchi, M.; Zhao, Y.; Lopez-Hilfiker, F.; Liu, J.; Shilling, J. E.; Xing, J.; Mathur, R.; Middlebrook, A. M.; Liao, J.; Welti, A.; Graus, M.;

https://doi.org/10.1021/acsestair.3c00037
ACS EST Air 2024, 1, 113−128

Warneke, C.; de Gouw, J. A.; Holloway, J. S.; Ryerson, T. B.; Pollack, I. B.; Thornton, J. A. Anthropogenic Enhancements to Production of Highly Oxygenated Molecules from Autoxidation. *Proc. Natl. Acad. Sci. U. S. A.* **2019**, *116* (14), 6641−6646.
(67) Vasquez, K. T.; Crounse, J. D.; Schulze, B. C.; Bates, K. H.; Teng, A. P.; Xu, L.; Allen, H. M.; Wennberg, P. O. Rapid Hydrolysis of Tertiary Isoprene Nitrate Efficiently Removes NOx from the Atmosphere. *Proc. Natl. Acad. Sci. U. S. A.* **2020**, *117* (52), 33011−33016.
(68) Xu, L.; Guo, H.; Boyd, C. M.; Klein, M.; Bougiatioti, A.; Cerully, K. M.; Hite, J. R.; Isaacman-VanWertz, G.; Kreisberg, N. M.; Knote, C.; Olson, K.; Koss, A.; Goldstein, A. H.; Hering, S. V.; de Gouw, J.; Baumann, K.; Lee, S.-H.; Nenes, A.; Weber, R. J.; Ng, N. L. Effects of Anthropogenic Emissions on Aerosol Formation from Isoprene and Monoterpenes in the Southeastern United States. *Proc. Natl. Acad. Sci. U. S. A.* **2015**, *112* (1), 37−42.
(69) Zhang, X.; Cappa, C. D.; Jathar, S. H.; McVay, R. C.; Ensberg, J. J.; Kleeman, M. J.; Seinfeld, J. H. Influence of Vapor Wall Loss in Laboratory Chambers on Yields of Secondary Organic Aerosol. *Proc. Natl. Acad. Sci. U. S. A.* **2014**, *111* (16), 5802−5807.
(70) Chowdhury, P. H.; He, Q.; Lasitza Male, T.; Brune, W. H.; Rudich, Y.; Pardo, M. Exposure of Lung Epithelial Cells to Photochemically Aged Secondary Organic Aerosol Shows Increased Toxic Effects. *Environ. Sci. Technol. Lett.* **2018**, *5* (7), 424−430.
(71) Liu, F.; Xu, T.; Ng, N. L.; Lu, H. Linking Cell Health and Reactive Oxygen Species from Secondary Organic Aerosols Exposure. *Environ. Sci. Technol.* **2023**, *57* (2), 1039−1048.
(72) Tuet, W. Y.; Chen, Y.; Fok, S.; Champion, J. A.; Ng, N. L. Inflammatory Responses to Secondary Organic Aerosols (SOA) Generated from Biogenic and Anthropogenic Precursors. *Atmospheric Chem. Phys.* **2017**, *17* (18), 11423−11440.
(73) Tuet, W. Y.; Chen, Y.; Fok, S.; Gao, D.; Weber, R. J.; Champion, J. A.; Ng, N. L. Chemical and Cellular Oxidant Production Induced by Naphthalene Secondary Organic Aerosol (SOA): Effect of Redox-Active Metals and Photochemical Aging. *Sci. Rep.* **2017**, *7* (1), 15157.
(74) Solomon, P. A.; Crumpler, D.; Flanagan, J. B.; Jayanty, R. K. M.; Rickman, E. E.; McDade, C. E. U.S. National PM2.5 Chemical Speciation Monitoring Networks—CSN and IMPROVE: Description of Networks. *J. Air Waste Manag. Assoc.* **2014**, *64* (12), 1410−1438.

https://doi.org/10.1021/acsestair.3c00037
ACS EST Air 2024, 1, 113−128